iScience

CellPress
OPEN ACCESS

Article

Δ42PD1-TLR4 Augments γδ-T Cell Activation of the Transitional Memory Subset of CD4$^+$ T Cells

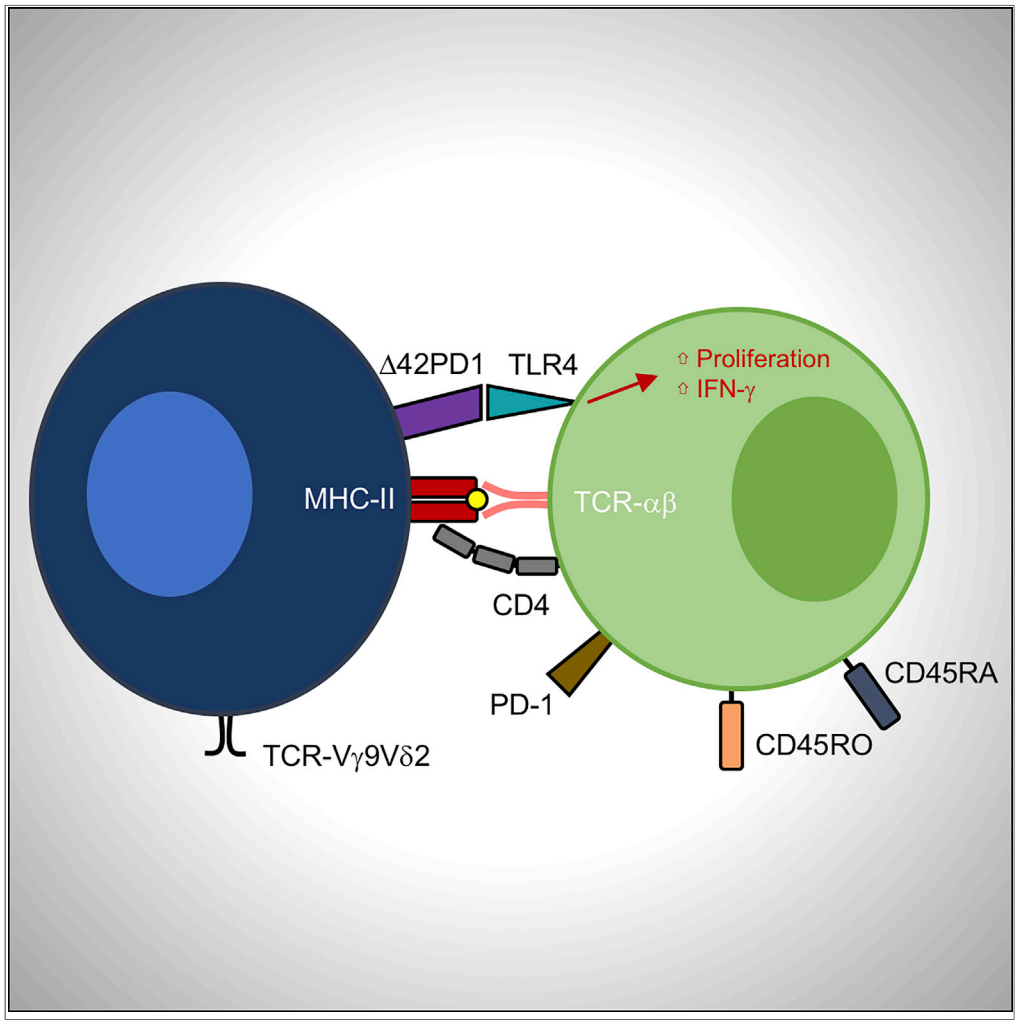

Yufei Mo, Allen Ka Loon Cheung, Yue Liu, Li Liu, Zhiwei Chen

akcheung@hkbu.edu.hk (A.K.L.C.)
zchenai@hku.hk (Z.C.)

HIGHLIGHTS

Δ42PD1 is co-expressed with MHC-II on activated Vδ2 cells

Δ42PD1$^+$MHC-II$^+$Vδ2 cells interact directly with TLR4$^+$CD4$^+$T cells in 3D imaging

TLR4 is highly expressed on the PD-1$^+$CD45RO$^+$ CD45RA$^+$CD4$^+$T cell subset

Δ42PD1-TLR4 selectively activates this subset of Ag-specific CD4$^+$ T cells

Mo et al., iScience *23*, 101620
October 23, 2020
https://doi.org/10.1016/j.isci.2020.101620

iScience

CellPress
OPEN ACCESS

Article

Δ42PD1-TLR4 Augments γδ-T Cell Activation of the Transitional Memory Subset of CD4$^+$ T Cells

Yufei Mo,[1,3] Allen Ka Loon Cheung,[2,3,4,*] Yue Liu,[2] Li Liu,[1] and Zhiwei Chen[1,*]

SUMMARY

TLR ligands can contribute to T cell immune responses by indirectly stimulating antigen presentation and cytokines and directly serving as co-stimulatory signals. We have previously reported that the human endogenous surface protein, Δ42PD1, is expressed primarily on (Vγ9)Vδ2 cells and can interact with TLR4. Since Vδ2 cells possess antigen presentation capacity, we sought to further characterize if the Δ42PD1-TLR4 interaction has a role in stimulating T cell responses. In this study, we found that stimulation of Vδ2 cells not only upregulated Δ42PD1 expression but also increased MHC class II molecules necessary for the antigen presentation. In a mixed leukocyte reaction assay, upregulation of Δ42PD1 on Vδ2 cells elevated subsequent T cell proliferation. Furthermore, the interaction between Δ42PD1-TLR4 augments Vδ2 cell stimulation of autologous CMV pp65-or TT-specific CD4$^+$ T cell proliferation and IFN-γ responses, which was specifically and significantly reduced by blocking the Δ42PD1-TLR4 interaction. Furthermore, confocal microscopy analysis confirmed the interaction between Δ42PD1$^+$HLA-DR$^+$Vδ2 cells and TLR4$^+$CD4 T cells. Interestingly, the subset of CD4$^+$ T cells expressing TLR4 appears to be PD-1$^+$ CD45RO$^+$CD45RA$^+$ transitional memory T cells and responded to Δ42PD1$^+$HLA-DR$^+$Vδ2 cells. Overall, this study demonstrated an important biological role of Δ42PD1 protein exhibited by Vδ2 antigen-presenting cells in augmenting T cell activation through TLR4, which may serve as an additional co-stimulatory signal.

INTRODUCTION

T cell activation occurs upon receiving signals from major histocompatibility complex (MHC) class I and II molecules for antigen presentation (signal 1), co-stimulatory molecules (signal 2), and cytokines (signal 3) (Kapsenberg, 2003). This process is carried out most efficiently by the classical professional antigen-presenting cell (APC), dendritic cell (DC), compared with other cell types. Although the co-stimulatory molecules from the B7 family govern the degree of T cell responses (Zou and Chen, 2008), Toll-like receptors (TLRs) as pattern recognition receptors (PRRs) in innate immunity have been shown to have a direct co-stimulatory effect on the activation of TLR-expressing T cells, such as TLR4 (Rahman et al., 2009). TLR4 complexes with CD14 and MD-2 on myeloid cells to produce pro-inflammatory cytokines in response to the foreign microbial membrane component lipopolysaccharide (LPS) (Zanoni et al., 2011), but they could also respond to endogenous danger associated molecular patterns (DAMPS), including heat shock protein 60 (HSP60) and high mobility growth box protein 1 (HMGB1) (Cohen-Sfady et al., 2005; Apetoh et al., 2007; Yang et al., 2010). So far, studies on the effect of TLR4 signaling on enhancing T cell function were performed using soluble adjuvants such as LPS and lipid A (Cairns et al., 2006; Gandhapudi et al., 2013; Reynolds et al., 2012; Zanin-Zhorov and Cohen, 2013). However, an endogenous surface expressed protein that could interact with TLR4 to affect T cell response has not been shown until recently on Vγ9Vδ2 cells, named Δ42PD1 (Cheung et al., 2017).

Human γδ-T cells consist of 0.5%–10% of peripheral blood lymphocytes and are composed of two subsets, Vγ9Vδ1 and Vγ9Vδ2 (hereafter referred to as Vδ1 and Vδ2 cells), with the latter being the predominant subpopulation (>80%) (Eberl et al., 2003; Evans et al., 2001). γδ-T cells differ from conventional αβ CD4$^+$ and CD8$^+$ T cells based on VDJ recombination with added variability of the complementary-determining region

[1]AIDS Institute and Department of Microbiology, State Key Laboratory of Emerging Infectious Diseases, Li Ka Shing Faculty of Medicine, The University of Hong Kong, L5-45, 21 Sassoon Road, Pokfulam, Hong Kong SAR, China

[2]Department of Biology, Faculty of Science, RRS833, Ho Sin-hang Campus, Hong Kong Baptist University, 224 Waterloo Road, Kowloon Tong, Hong Kong SAR, China

[3]These authors contributed equally

[4]Lead Contact

*Correspondence: akcheung@hkbu.edu.hk (A.K.L.C.), zchenai@hku.hk (Z.C.)

https://doi.org/10.1016/j.isci.2020.101620

3 (CDR3) of the expressed T cell receptor (TCR) during thymocyte development (Girardi, 2006). Vδ2 cells are considered as the bridge between innate and adaptive immune responses based on their ability to present not only antigens but also rapid (pro-inflammatory) cytokine and chemokine responses (Vantourout and Hayday, 2013). These cells become activated in recognition of nonpeptide phosphoantigens derived from bacteria (Tanaka et al., 1994). However, cognate isopentenyl pyrophosphate (IPP), which is an intermediate product of the mevalonate pathway, could also stimulate Vδ2 cells (Gober et al., 2003). In addition, the butyrophilin (BTN)3A1 and BTN2A1 molecules appear to be important in the activation of the cytolytic function of Vδ2 cells (Harly et al., 2012; Vavassori et al., 2013; Rigau et al., 2020). The Vδ2 subset possesses ample antigen presentation capacity comparable with DC (Brandes et al., 2005, 2009; Moser and Brandes, 2006; Meuter et al., 2010; Moser and Eberl, 2007). Interestingly, recent reports have shown that Vδ2 cells can present viral antigens from Epstein-Barr virus (EBV), influenza virus, measles virus, *Mycobacterium tuberculosis*-purified protein derivative (PPD), and single chain tetanus toxoid protein (Bieback et al., 2003; Brandes et al., 2005, 2009; Meuter et al., 2010; Landmeier et al., 2009; Tyler et al., 2017; Hu et al., 2012). In some cases, Vδ2 cells are more efficient than DC as APC, such as the process of cross-presentation to $CD8^+$ T cells (Brandes et al., 2009), which highlights a unique niche of these cells in stimulating adaptive T cell response. Till now, however, no evidence has shown that TLR4 is associated with the co-stimulation function exerted by Vδ2 cells on T cells.

We recently identified an isoform of human programmed death 1 (PD-1) as a 42-nucleotide deletion variant (Δ42PD1) expressed on Vδ2 cells, which does not bind PD-L1/L2 but can interact with and induce TLR4 downstream signaling (Zhou et al., 2013; Cheung et al., 2017). To further characterize the function of Δ42PD1-TLR4, we examined T cell activation that could be induced by $\Delta42PD1^+$Vδ2 cells. Our data showed that Δ42PD1 expression was accompanied by MHC class II upregulation on activated Vδ2 cells, which led to the hypothesis that Δ42PD1 may augment $CD4^+$ T cell activation to promote antigen presentation. By performing a classical mixed leukocyte reaction (MLR) assay, we found that Δ42PD1 can enhance the antigen presentation ability of Vδ2 cells to stimulate naive T cell response via TLR4, which was further shown with responses against pp65 antigen of human cytomegalovirus (CMV) and tetanus toxin (TT). The interaction between $\Delta42PD1^+$Vδ2 cells and $TLR4^+CD4^+$ T cells was observed through confocal microscopy. Furthermore, we found that TLR4 was primarily expressed by $PD\text{-}1^+$ T cell subset with $CD45RA^+CD45RO^+$ phenotype that can respond to $\Delta42PD1^+$Vδ2 cells. Taken together, our data demonstrated an unrecognized immune pathway specific for the activation of a memory T cell subset by Vδ2 cells augmented by Δ42PD1-TLR4.

RESULTS

Δ42PD1 Is Co-expressed with MHC Class II on Vδ2 Cells

Our previous data showed that various virus infections can induce Δ42PD1 expression on Vδ2 cells (Cheung et al., 2017). To further characterize the requirement for the upregulation of Δ42PD1 expression, a panel of cytokines was used to determine if direct treatment of purified γδ-T cells can induce Δ42PD1 expression. IFN-β, IFN-γ, IL-2, IL-10, IL-12, IL-15, IL-18, IL-12/IL-15, and IL-12/IL-18 were used for 5 days of stimulation. By flow cytometry, the highest significant Δ42PD1 upregulation was found for IL-12/IL-15 and IL-12/IL-18 (Figure 1A). The induction of activation marker CD69 expression by IL-12/IL-15 was found greater than IL-12/IL-18 (Figure S1). Next, we examined if Vδ2 cells upregulated MHC class II (HLA-DR) following cytokine stimulation. IL-2, IL-12, IL-12/IL-15, and IL-12/IL-18 upregulated the HLA-DR significantly, where IL-12/IL-15 appears to have the highest level of induction on $CD3^+V\delta2^+$ cells and greater than IL-12/IL-18 (Figure 1B). Moreover, IL-12/IL-15 stimulated the largest proportion of cells co-expressing Δ42PD1 and HLA-DR (Figures 1C and 1D). Therefore, IL-12/IL-15 appears to be the best cytokine combination in activating $\Delta42PD1^+$Vδ2 cells with potential upregulated MHC-II molecules for antigen presentation. Moreover, IL-12/IL-15 did not significantly alter the ratio of Vδ1/Vδ2 cells (Figure S2). In addition, under viral infections of PBMCs, Vδ2 cells upregulated HLA-DR expression at 3 days post infection (P.I.) by each of the viruses, where Δ42PD1 was exclusively expressed on $HLA\text{-}DR^+$ cells with statistical significance (Figures 1E and S3). CMV infection is known to induce an increased proportion of $V\delta1^+$ subset in transplant recipients over time (Pitard et al., 2008; Dechanet et al., 1999). Therefore, we sought to see if *in vitro* CMV infection of PBMCs in 3 days could induce Vδ1 cells, but no significant changes in either the proportion of Vδ1/Vδ2 cells or Δ42PD1 expression on Vδ1 cells were found (Figures S4A–S4C).

Δ42PD1 Augments γδ-T Cells Stimulation of $CD4^+$ T Cells

To determine whether $\Delta42PD1^+$ Vδ2 cells can enhance T cell activation, we performed a proof-of-concept MLR experiment. PBMCs from one healthy human donor served as stimulator treated with γ-irradiation and

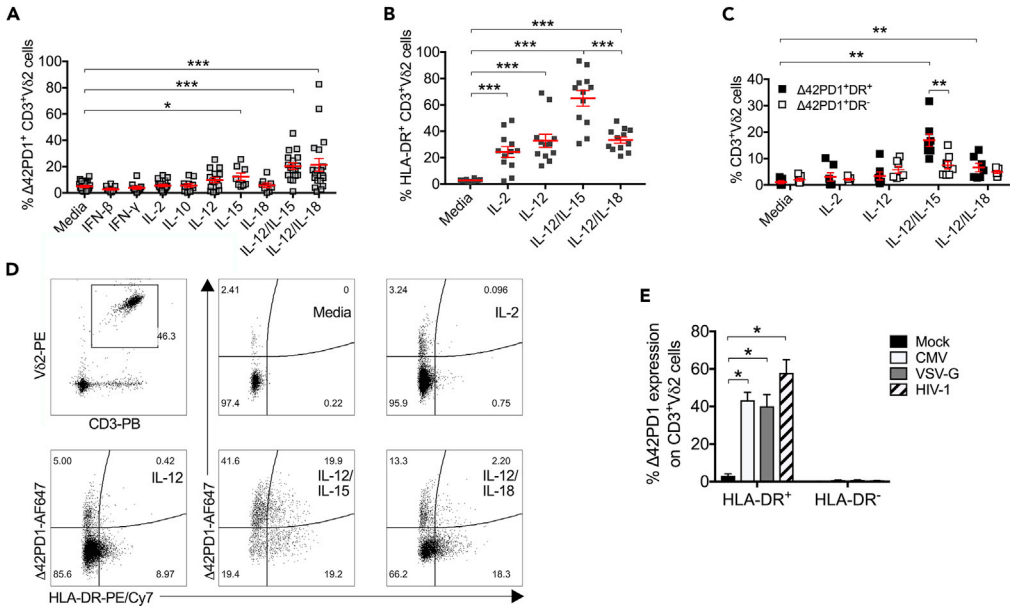

Figure 1. Δ42PD1 and HLA-DR Expression on Cytokine-Stimulated CD3$^+$Vδ2$^+$ Cells

Purified γδ-T cells from healthy PBMCs were isolated and stimulated with different cytokines for 5 days and analyzed for the expression of (A) Δ42PD1, (B) HLA-DR, and (C) co-expression of Δ42PD1/HLA-DR by flow cytometry ($n \geq 8$). (D) Representative flow cytometry dot plots of Δ42PD1/HLA-DR co-expression on CD3$^+$Vδ2$^+$ cells, or as column graphs are shown ($n = 4$) (E). Data are shown as mean ± SEM. *$p < 0.05$, **$p < 0.01$, ***$p < 0.001$. See also Figures S1–S4.

then were co-cultured with PBMCs from an allogeneic donor to measure CFSE-labeled cell proliferation (effectors). To test the specific relevance of Δ42PD1, donor cells were pre-treated with anti-Δ42PD1 (CH101), or effector cells were treated with anti-TLR4 blocking antibody, or relevant isotype antibodies. Effector PBMCs depleted for γδ-T cells, unstimulated cells (negative control) or PHA/IL-2-stimulated cells (positive control) were used for comparison. After 5 days, ~20% of effector cells showed proliferation in the isotype antibody group (Figures 2A and 2B). Interestingly, effector PBMCs with γδ-T cells depleted had proliferation 2-fold less than intact PBMCs. Blocking of TLR4 or Δ42PD1 halved the proliferative response significantly, whereas Transwell setup abrogated the response (Figures 2A and 2B). Therefore, these results suggest that γδ-T cells and Δ42PD1-TLR4 play a role in stimulating T cell response. To verify if Δ42PD1 can be induced on Vδ2, effector purified γδ-T cells of one donor were treated with irradiated allogeneic donor PBMCs for 1 and 5 days. An increased level of Δ42PD1 that co-expressed with HLA-DR and CD83 was found on a small proportion of cells (Figures S5A–S5C). However, by day 5 post treatment, the co-expression of HLA-DR and CD83 molecules was no longer significant albeit increased Δ42PD1. Next, purified γδ-T cells treated with irradiated allogeneic PBMCs for 1 day were then co-cultured with autologous purified CFSE-labeled naive CD4$^+$ as the effector cells. As a result, an elevated level of CD4 T cell proliferation was observed (~15%), which was subdued by around half in the presence of blocking antibody against Δ42PD1 or TLR4 (Figure 2C).

To further show the relevance of Δ42PD1-TLR4 in CD4$^+$ T cell stimulation, a proliferation experiment was performed in the absence of antigen. γδ-T cells stimulated with IL-12/IL-15 for 5 days were co-cultured with autologous CFSE-labeled CD4$^+$ T cells for another 5 days to assess proliferation. As shown in Figure 2D, IL-12/IL-15 treatment of γδ-T cells could stimulate on average 12% of CD4$^+$ T cells to proliferate and the effect was inhibited by anti-Δ42PD1. Unstimulated DC or γδ-T cells had no effect on CD4$^+$ T cells. These data demonstrate that γδ-T cells could stimulate CD4$^+$ T cell responses to a certain degree mediated by Δ42PD1 without antigen.

CMV is a ubiquitous beta-herpesvirus that induces "memory inflation" in the human population for increased antigen-specific T cells (Klenerman and Oxenius, 2016); we made use of this fact to test the relevance of Δ42PD1-TLR4 in stimulating CMV-specific T cell responses. PBMCs were first stimulated with CMV antigen pp65 (gB; viral phosphoprotein encoded by UL83) peptide pool/IL-2 for one week to expand

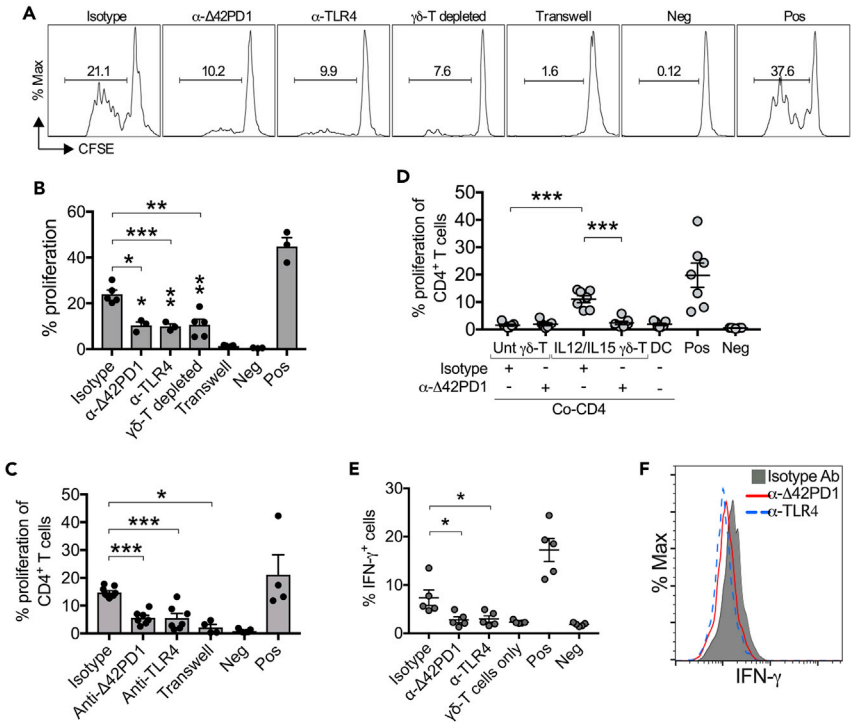

Figure 2. Δ42PD1-TLR4 Augments CD4$^+$ T Cell Stimulation by γδ-T Cells

Mixed leukocyte reaction assay between allogeneic PBMCs was performed in the presence of isotype, anti-Δ42PD1, anti-TLR4 antibodies or depleted for γδ-T cells (n = 4). For non-specific antigen stimulation, γδ-T cells were stimulated with γ-irradiated PBMC from an allogeneic donor at a 1:10 ratio, or co-cultured with autologous CFSE-labeled total CD4$^+$ cells at a ratio of 1:1 for 5 days, in the presence of isotype, anti-Δ42PD1, anti-TLR4 antibodies. Transwell was used to separate γ-irradiated PBMC-stimulated γδ-T cells and effector cells. Proliferation was measured by flow cytometry based on CFSE signals.

(A and B) (A) Representative CFSE proliferation flow cytometric histograms (numbers indicate percentages), or as (B) column graphs are shown (n = 4).

(C) MLR with CFSE-labeled CD4$^+$ T cell proliferation (n ≥ 4).

(D) CFSE proliferation of autologous CD4$^+$ T cell proliferation induced by IL-12/IL-15-stimulated γδ-T cells (n = 7).

(E and F) (E) γδ-T cells were isolated from CMV-infected PBMCs at day 3 P.I. before being co-cultured (1:5) with pp65 peptide-stimulated autologous T cells to assess intracellular IFN-γ (n = 5), where (F) shows representative overlaid histograms. Neg, unstimulated effector cells; Pos for (A)–(D), PHA/IL-2 stimulation; Pos for (E) PMA/ionomycin. Data represent mean ± SEM. *p < 0.05, **p < 0.01, ***p < 0.001.

See also Figures S5 and S6.

pp65-specific T cells similar to previous studies (Brandes et al., 2009; Rauser et al., 2004). Then, autologous γδ-T cells isolated from CMV-infected PBMCs were used to activate pp65-specific T cells by co-culture (1:5). By flow cytometry analysis, up to 10% of CD4$^+$ T cells were found to produce IFN-γ (Figure 2E). These effects, however, were significantly reduced when anti-Δ42PD1 or anti-TLR4 blocking antibodies were used (Figures 2E and 2F). In addition, to remove the possibility that media containing fetal bovine serum (FBS) components could lead to background cell activation, we performed proliferation and IFN-γ experiments using AIM-V serum-free media, and the same trend of results was observed (Figure S6). Taken together, the data so far indicate that CD3$^+$Vδ2$^+$ cells are capable of antigen presentation and antigen-specific CD4$^+$ T cell activation, which is enhanced upon Δ42PD1-TLR4 interaction.

Δ42PD1$^+$HLA-DR$^+$ Vδ2 Cells Interact with Antigen-Specific TLR4$^+$CD4 T Cells

Next, we sought to verify that Δ42PD1-TLR4 can interact between Vδ2 cells and antigen-specific CD4 T cells using confocal microscopy. pp65-Specific CD4$^+$ T cells were used to co-culture with autologous IL-12/IL-15 stimulated and pp65-pulsed γδ-T cells or untreated γδ-T cells for ~18 h before being analyzed. First, we found that the expression of Δ42PD1, γδ-TCR, and HLA-DR were co-localized on IL-12/IL-15-stimulated γδ-T cells (Figure S7A). Second, pp65-activated CD4$^+$ T cells expressed surface TLR4 and HLA-DR

(Figure S7B). Note that Vδ2 cells also expresses TLR4 (Figure S7C). Third, co-culture of pp65-specific $CD4^+$ T cells with unstimulated γδ-T cells resulted in no clustering of cells and minimal detection of Δ42PD1 expression (Figure 3A). In contrast, pp65-specific $CD4^+$ T cells formed cell clusters with IL-12/IL-15-stimulated $\Delta42PD1^+HLA\text{-}DR^+$ γδ-T cells, where Δ42PD1 and TLR4 appear to be in close proximity (Figure 3B). Fourth, further analysis confirmed that expressions of Δ42PD1 and HLA-DR were co-localized on stimulated Vδ2 cells but not on unstimulated cells (Figure 3C). Fifth, examining the expression profiles of Δ42PD1, HLA-DR, and TLR4 across multiple cell-cell interfaces suggests close interactions between these proteins on $\Delta42PD1^+HLA\text{-}DR^+V\delta2$ and $TLR4^+CD4^+$ T cells (Figure 3D; Videos S1 and S2). Sixth, z-stack analysis showed that $\Delta42PD1^+HLA\text{-}DR^+V\delta2$ and $TLR4^+CD4^+$ T cells are interacting inside the cell clusters when examined orthogonally at the XZ and XY axes (Figure 3E; *crosshairs*). Lastly, Imaris software was used to construct a 3D model to better demonstrate the interaction between $\Delta42PD1^+HLA\text{-}DR^+V\delta2$ and $TLR4^+CD4^+$ T cells at the cell-cell interface (Figure 3F; Video S3).

$PD\text{-}1^+CD4^+$ T Cells Exhibit High Expression of TLR4

Previous studies have reported the role of TLR4 signaling in T cell response (González-Navajas et al., 2010; Reynolds et al., 2012; Tripathy et al., 2017; Zanin-Zhorov and Cohen, 2013; Zanin-Zhorov et al., 2007). TLR4-adjuvants such as monophosphoryl lipid A (MPLA) and LPS appear to act on and induce greater OVA-specific T cell clonal expansion in mice compared with OVA alone, suggesting that TLR4 signaling could augment T cell response (Mata-Haro et al., 2007; Gandhapudi et al., 2013). From the above data, we showed a contributing role of Δ42PD1-TLR4 in activating $CD4^+$ T cell responses. To further investigate this, it is necessary to confirm that $CD4^+$ T cells do express surface TLR4. By flow cytometry, we measured TLR4 expression among healthy door PBMCs (n = 25) and found that a subset of ~5% of purified total $CD4^+$ T cells are $TLR4^+$, which are majorly found on the $PD\text{-}1^+$ subpopulation when compared with $PD\text{-}1^-$ (Figures 4A and 4B). By western blotting, we confirmed the expression of TLR4 protein in purified $CD4^+$ T cells compared with positive control cell lines transiently (293T-TLR4) or stably expressing TLR4 (HEKBlue-hTLR4) (Figure 4C). Upon activation by anti-CD2/anti-CD3/anti-CD28 antibodies (referred to as anti-CD2/3/28 hereafter) on purified $CD4^+$ T cells for 5 days, higher proportion of $TLR4^+$ cells were found on $PD\text{-}1^+$ cells compared with $PD\text{-}1^-$ cells (Figures 4D and 4E). An increase in TLR4 protein expression was also detected by western blotting from day 3 activated $CD4^+$ T cells isolated from three independent donors (Figure 4F). Furthermore, western blotting of FACSorted $TLR4^+$ cells following activation showed higher TLR4 protein detection than $TLR4^-$ cells (Figures 4G and 4F). MOLT4 cell line showed a lower level of TLR4 compared with stably expressing HEKBlue-hTLR4 cells (Figures 4G, 4H, and S8A). To understand the detection of TLR4 in both sorted $TLR4^+$ and $TLR4^-$ cell subpopulations, intracellular flow cytometry analysis showed an increased detection of TLR4 expression compared with surface staining (Figure S8B). In addition, confocal microscopy also showed an increase in cytoplasmic TLR4 in stimulated $CD4^+$ T cells (Figure S8C). These results confirmed that TLR4 is indeed expressed by $CD4^+$ T cells following activation.

$CD45RA^+CD45RO^+PD\text{-}1^+$ $CD4^+$ T Cells Highly Express Surface TLR4 and Respond to $\Delta42PD1^+V\delta2$ Cells

To identify the $CD4^+$ T cell subset expressing PD-1 and TLR4, we performed flow cytometry using additional markers CD45RA and CD45RO. Total $CD4^+$ T cells isolated from healthy donors were unstimulated (media) or stimulated with IL-2, PHA/IL-2, or anti-CD2/3/28 antibodies for 3 days. By flow cytometry, the proportion of $CD45RO^+CD45RA^+$ subset of $CD4^+$ T cells increased up to ~13% with stimulation compared with ~4% in the media control (Figures 5A and S9). The $CD45RO^-CD45RA^+$ naive $CD4^+$ T cell subset remained at around 40%, whereas $CD45RO^+CD45RA^-$ cells appear to have slightly decreased upon PHA/IL-2 or anti-CD2/3/28 stimulation and the $CD45RO^+CD45RA^+$ subset increased modestly (Figures 5A and S9). Moreover, TLR4 was found majorly expressed on the $CD45RO^+CD45RA^+PD\text{-}1^+$ cells compared with their $PD\text{-}1^-$ counterparts or other subsets (Figures 5B and S10). In addition, $CD45RO^+CD45RA^+$ CCR7-positive but not CCR7-negative cells harbored TLR4 expression (Figure S11).

To demonstrate that $CD45RO^+CD45RA^+PD\text{-}1^+$ $CD4^+$ T cells with antigen-specificity can respond to $\Delta42PD1^+V\delta2$ cells, we performed co-culture experiment using tetanus toxin protein fragment C (TT) as the antigen (Corinti et al., 1999). Purified γδ-T cells were activated with IL-12/IL-15, with or without γ-irradiated Raji B cells, or with IPP/IL-2, followed by incubation with no antigen or with TT. However, IPP/IL-2 did not induce Δ42PD1 and HLA-DR co-expression on Vδ2 cells (Figure S12A). Raji cells served as feeder cells during the antigen presentation process of Vδ2 cells to better upregulate co-stimulatory molecules CD40, CD80, CD86 (Brandes et al., 2003, 2005). Autologous total $CD4^+$ T cells were co-cultured with these

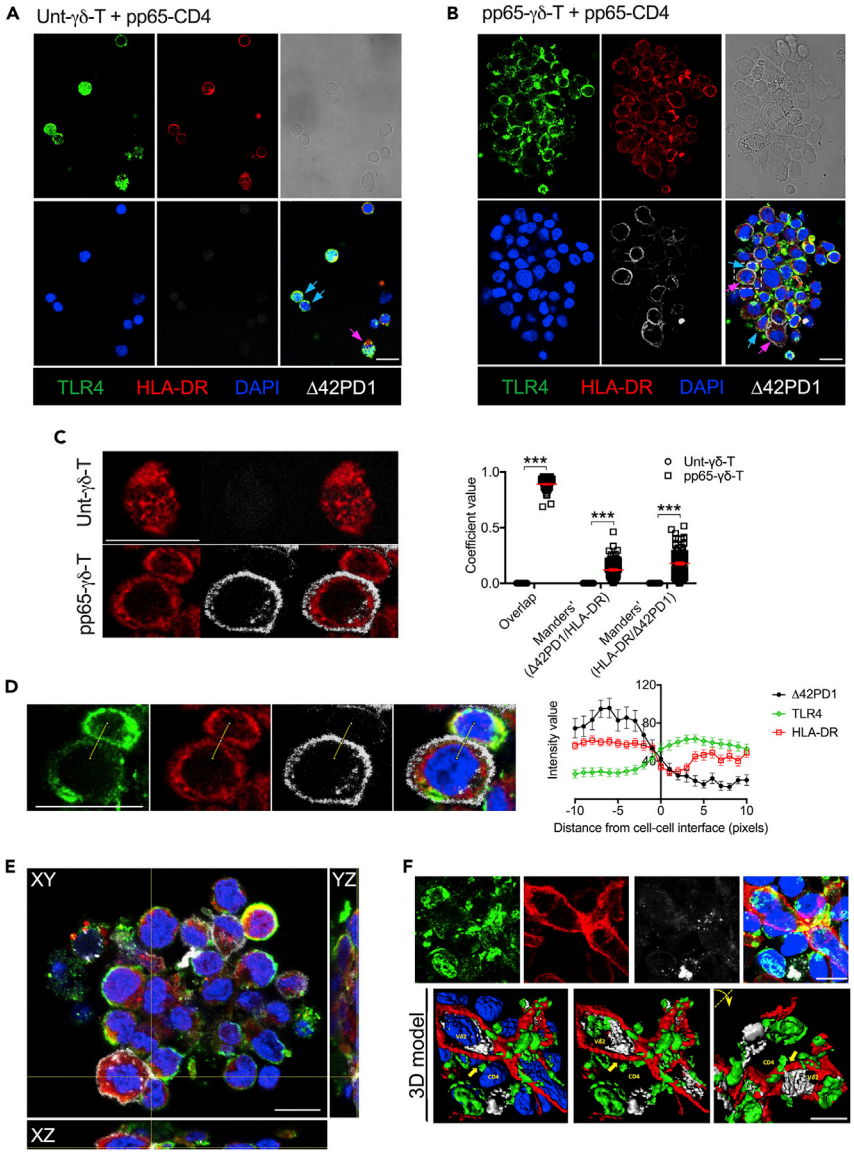

Figure 3. Δ42PD1-TLR4 Interaction between Vδ2 and CD4$^+$ T Cells

pp65-Specific CD4$^+$ T cells were used to co-culture with autologous IL-12/IL-15 stimulated and pp65-pulsed γδ-T cells or untreated (Unt) γδ-T cells for around 18 h, before being fixed and immunostained for Δ42PD1 (white), TLR4 (green), HLA-DR (red), and DAPI (blue). Co-culture of pp65-specific CD4$^+$ T cells with (A) unstimulated γδ-T cells or (B) with IL-12/IL-15 stimulated and pp65-pulsed γδ-T cells. Pink and blue arrows point to Δ42PD1$^+$HLA-DR$^+$ and TLR4$^+$ cells, respectively. Pixel size = 120.2 nm.

(C) Representative images showing colocalization of Δ42PD1 and HLA-DR expression signals on Unt (n = 65) and pp65-pulsed γδ-T cells (n = 96) were analyzed, for the overlap and Manders' coefficient values shown in the graph.

(D) Representative images showing the interaction between pp65-specific CD4$^+$ T cell and pp65-pulsed γδ-T cells analyzed by the signal values for Δ42PD1, MHC-II, and TLR4 along the yellow line transecting from bottom left to top right equivalent to left to right in the histogram. Values are indicated by the histogram of n = 32 cell-cell pairs at ten pixels before and after interface between the cells set at x = 0.

(E) Orthogonal views over XY, XZ, and YZ axes of a z-stack of 78 images at 0.29 μm thickness each. Image at stack 72 is shown for the interaction between pp65-specific CD4$^+$ T cell and pp65-pulsed γδ-T cells. Pixel size = 80.2 nm.

(F) Imaris analysis on a maximum projection of a z-stack of 25 images each with a thickness of 0.506 μm (top) to generate the 3D model (bottom). Pixel size = 112 nm. The rightmost image is a flipped version of the middle image to indicate interactions at two different angles. White bar represents a scale of 10 μm. Representative images from three independent experiments are shown. Data in the graphs represent mean ± SEM. ***$p < 0.001$.

See also Figure S7, Videos S1, S2, and, S3.

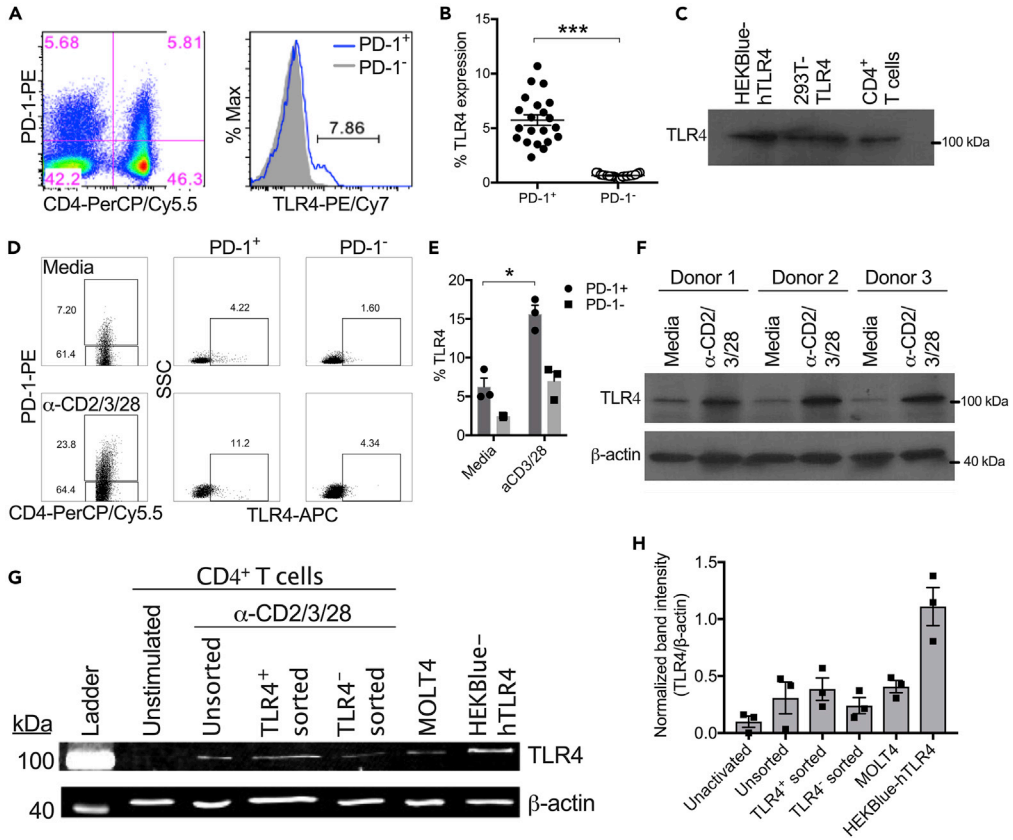

Figure 4. TLR4 Is Expressed on CD4$^+$ T Cells

PBMC samples were analyzed by flow cytometry for surface TLR4 expression on PD-1$^+$ or PD-1$^-$ CD4$^+$ T cells.

(A and B) (A) Representative flow cytometry analysis plots on unstimulated PBMCs from n = 21 independent donor samples (B).

(C) ECL western blotting detection of TLR4 protein from freshly PBMC-isolated CD4$^+$ T cells, stable expression cell line HEKBlue-hTLR4, and transiently expressed TLR4 on 293T cells.

Purified total CD4$^+$ T cells stimulated with anti-CD2/3/28 antibodies were analyzed for TLR4 expression with representative plots shown (D) or as a graph for n = 3 independent donors (E), confirmed by ECL western blotting (F).

(G) Detection of TLR4 and β-actin in FACSorted TLR4$^+$ and TLR4$^-$ cells after anti-CD2/3/28 activation by Fluorescent western blotting compared with unsorted, unstimulated media control, and control cell lines. Representative blot from one of three donors shown. Ladder markers for (C) and (F) are indicated on the side. (H) Normalized band density (normalizing band density of TLR4 to that of β-actin) was calculated and compared. Column graph data represent mean ± SEM. *$p < 0.05$, ***$p < 0.001$.

See also Figure S8.

stimulated γδ-T cells for 24 h and assessed for intracellular IFN-γ expression in the CD45RO$^+$CD45RA$^+$PD-1$^+$ subset (Figure S12B). Without antigen, stimulated γδ-T cells modestly activated CD45RO$^+$CD45RA$^+$PD-1$^+$ cells similar to the results in Figure 3. TT alone had little effects in stimulating CD4$^+$ T cells in the two donors we tested, whereas IL-12/IL-15-treated cells pulsed with TT stimulated ~10% of IFN-γ$^+$ CD45RO$^+$CD45RA$^+$PD-1$^+$ cells. In the presence of Raji cells, the level of stimulated cells increased to ~17%, indicating that the feeder cells increased the effectiveness as reported previously (Himoudi et al., 2012) (Figure S12B). In comparison, IPP/IL-2-stimulated γδ-T cells with TT was relatively less capable in the induction of IFN-γ$^+$ CD45RO$^+$CD45RA$^+$PD-1$^+$ cells. Consistently, the addition of antibodies against Δ42PD1-TLR4 pathway appears to inhibit stimulated γδ-T cells in the activation of CD45RO$^+$CD45RA$^+$PD-1$^+$ cells (Figure S12B).

Next, we performed similar experiments using another antigen, CMV pp65 (Figures 5C and S13). γδ-T cells treated with IL-12/IL-15/Raji cells and pulsed with pp65 protein were used to stimulate pp65-specific T cells in a co-culture experiment. As expected, CD4$^+$CD45RO$^+$CD45RA$^+$PD-1$^+$ cells showed increased IFN-γ

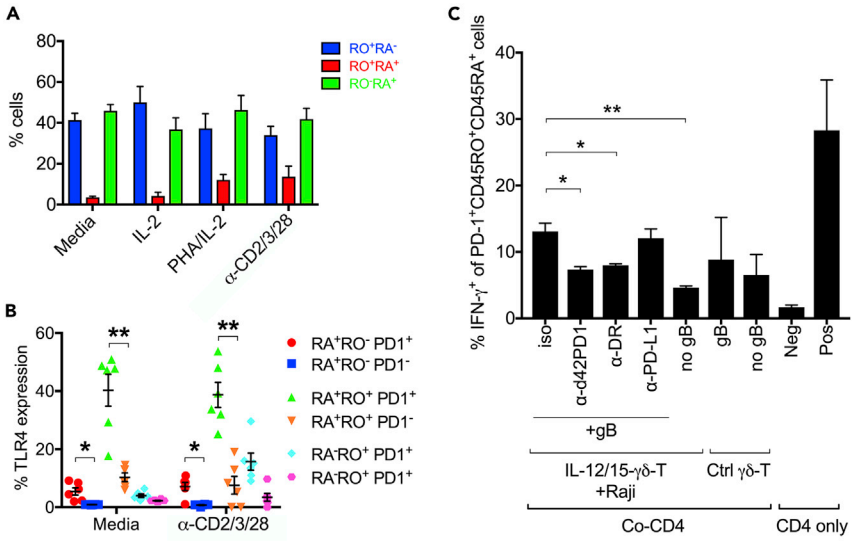

Figure 5. Preferential Response of TLR4$^+$PD-1$^+$CD45RO$^+$CD45RA$^+$ T Cell Subset to Activation by Δ42PD1$^+$Vδ2 cells

(A) PBMCs stimulated for 3 days with IL-2, PHA/IL-2, anti-CD2/3/28 antibodies, or left in media, were analyzed by flow cytometry for the frequencies of CD45RO/CD45RA subsets of CD4$^+$ T cell ($n \geq 6$).

(B) TLR4 expression assessed on PD-1$^+$ or PD-1$^-$ subsets of CD45RO/CD45RA CD4$^+$ T cells ($n = 6$).

(C) Intracellular IFN-γ response of CD45RO$^+$CD45RA$^+$CD3$^+$CD4$^+$ T cells stimulated by γδ-T cells treated with IL-12/IL-15/Raji with or without pp65, in the presence of isotype, anti-Δ42PD1, anti-HLA-DR, or anti-PD-L1 antibody. CD4$^+$ T cells treated with PMA/ionomycin (Pos) or media (Neg) served as controls. Four independent experiments were performed. Data represent mean ± SEM. *$p < 0.05$, **$p < 0.01$.

See also Figures S9–S13.

production (Figure 5C), which was significantly and consistently decreased when antibodies against Δ42PD1 or HLA-DR were used. CD45RO$^+$CD45RA$^-$ or CD45RO$^-$CD45RA$^+$ IFN-γ response was not affected by blocking Δ42PD1-TLR4 (Figures S13B and S13C). Interestingly, no increase in IFN-γ response was found when anti-PD-L1 antibody was used, suggesting that CD4$^+$CD45RO$^+$CD45RA$^+$PD-1$^+$ cells may not be "exhausted" or that the PD-1/PD-L1 pathway may not play a role in the context of Δ42PD1$^+$Vδ2 cells antigen presentation and stimulation of CD45RO$^+$CD45RA$^+$PD-1$^+$ cells. Without pp65 protein added or IL-12/IL-15/Raji stimulation, γδ-T cells were inefficient in triggering IFN-γ response from CD45RO$^+$CD45RA$^+$PD-1$^+$ cells. Overall, the data demonstrate that Δ42PD1$^+$Vδ2 cells can activate the specific TLR4$^+$PD-1$^+$ CD45RO$^+$CD45RA$^+$CD4$^+$ T cells.

DISCUSSION

In this study, we describe for the first time a mechanism for Δ42PD1 in augmenting the activation of a subset of T cells through TLR4 signaling upon stimulation by Vδ2 cells. Our data first defined the PD-1$^+$ subset of CD45RO$^+$CD45RA$^+$ CD4$^+$ T cells expressing high level of TLR4, which are responsive to the activation by Δ42PD1$^+$Vδ2 cells in an antigen-dependent manner. Blocking of the Δ42PD1-TLR4 pathway in this context significantly reduced CD45RO$^+$CD45RA$^+$ CD4$^+$ T cell IFN-γ responses. Therefore, Δ42PD1-TLR4 is likely an unrecognized co-activation signal that is unique to the TLR4$^+$PD-1$^+$CD45RO$^+$CD45RA$^+$ CD4$^+$ T cells.

The influence of Δ42PD1 on cell-mediated immunity is dependent on the fact that both CD4$^+$ and CD8$^+$ αβ-T cells express TLR4 (Caramalho et al., 2003; Komai-Koma et al., 2004, 2009; Zanin-Zhorov et al., 2007), where signaling through TLR4 in addition to antigen recognition could enhance T cell response (Caramalho et al., 2003; Reynolds et al., 2012). However, it has remained controversial as these previous studies utilized soluble TLR agonists to determine their effect on T cells, which may not reflect the difference to endogenous molecule(s). One recent study describing a computational approach defined TLR5 playing a co-stimulatory role in conjunction to TCR for T cell responses (Rodriguez-Jorge et al., 2019), which supports the notion that TLR can influence T cell activation. In this regard, since Δ42PD1 is the first endogenous surface protein found to interact with TLR4 (Cheung et al., 2017), it may have a unique niche function in

stimulating T cell responses. First, we found that Δ42PD1$^+$Vδ2 cells could induce proliferation of T cells through cell-cell interaction by Δ42PD1-TLR4 to augment T cell response (Figures 2, 3, and, S7). Second, in the presence of antigen, co-culture experiments also showed similar results but proliferation and IFN-γ production were decreased when Δ42PD1-TLR4 pathway was inhibited (Figures 2 and 5). These data confirmed not only that Vδ2 cells do indeed engage in antigen presentation but also that Δ42PD1-TLR4 serves to provide an additional co-stimulatory signal to T cell activation, which may be exclusive to TLR4-expressing T cells.

Post-activated CD4$^+$ T cells can express TLR4. Other studies have also suggested that activated and memory T cells could increase TLR4 for the purpose of enhanced responses (Cairns et al., 2006). Our data also confirmed that activation of T cells can lead to an increased level of TLR4 expression (Figures 4 and S8), but the subset of CD4$^+$ T cells that upregulated TLR4 needs to be identified. Therefore, by analyzing the CD45RA, CD45RO, and PD-1 markers to delineate the naive and memory subsets of CD4$^+$ T cells, we found that TLR4 is expressed on CD45RO$^+$CD45RA$^+$ subset of CD4$^+$ T cells that co-express PD-1 or CCR7 (Figures 5, S10, and S11). Upon T cell activation, CD45RA$^+$CD45RO$^-$ naive T cells acquire the CD45RA$^+$CD45RO$^+$ phenotype, which would receive further signals to progress into activated memory T cells, which is regarded as an intermediate phase or transitional memory T cells, but it could revert to naive cells if such signals are absent (Summers et al., 1994; Johannisson and Festin, 1995). Other studies have also identified this phenotype of memory T cells existing in the periphery that appears to have greater activation potential (Summers et al., 1994; Picker et al., 1993; Johannisson and Festin, 1995; Hamann et al., 1996; Baars et al., 1995). Therefore, it is possible that the expression of TLR4 allows the T cells to receive such signals from endogenous Δ42PD1 to become activated memory cells. However, in patients with chronic arthritis, the CD45RA$^+$CD45RO$^+$ subset of T cells composed 28%–30% of peripheral T lymphocytes, which underlies the autoimmune nature in the joints. Coincidentally, elevated levels of activated Vδ2 cells were also found in these patients (Mo et al., 2017; Bank et al., 2002). In contrast, HIV-1 gp120 exposed to CD4$^+$ T cells can induce the CD45RO$^+$CD45RA$^+$ phenotype and undergo apoptosis instead of forming the effector memory subset (Trushin et al., 2009), which may be one mechanism for the loss of CD4$^+$ T cells in patients with HIV-1. Although Δ42PD1-TLR4 signaling affects T cell activation and differentiation into a niche memory phenotype, it may also have a detrimental effect under autoimmune diseases condition (Jin et al., 2012).

It is interesting that TLR4 was not found to be expressed on all CD45RO$^+$CD45RA$^+$ but mainly on the PD-1$^+$ subset. Although PD-1 is well characterized for its function in the induction of T cell exhaustion, it is also recognized as an activation marker and as part of the memory phenotype (Ahn et al., 2018; Simon and Labarriere, 2017; Allie et al., 2011). Following activation, naive T cells could upregulate PD-1 within 1 day of antigen stimulation, which is accompanied by the expression of IFN-γ, granzyme B, and TNF-α by 2 days (Ahn et al., 2018). However, these studies did not evaluate the expression of TLR4 and its association with the PD-1$^+$ phenotype, which may be a critical step in further developing the cells into a memory phenotype or for a rapid memory-to-effector response. In addition, our findings suggest that the PD-1$^+$CD45RO$^+$CD45RA$^+$ subset may not be functionally exhausted, as anti-PD-L1 treatment did not increase the IFN-γ response (Figure 5). Thus, future characterization of this particular subset of T cells should be performed in relation to the requirement of TLR4 signaling for co-activating T cell function.

Taken together, this study demonstrated a unique cell-to-cell interacting protein couple that acts cohesively in a specialized manner in T cell activation. It is intriguing that the development of activated memory CD4$^+$ T cells, or that the triggering of memory T cell response in the early stages of reinfection, may require Δ42PD1$^+$Vδ2 cells. Our findings of the contribution of Δ42PD1-TLR4 pathway in the context of CD4$^+$ T cell activation suggests the role of endogenous TLR4 signaling in these immunological events. The downstream signaling pathway in the activation of TLR4$^+$ PD-1$^+$CD45RO$^+$CD45RA$^+$CD4$^+$ transitional memory T cells to progress into the activated memory phenotype remains to be elucidated.

Limitations of Study

Although we have demonstrated that the Δ42PD1-TLR4 pathway contributes to the activation of TLR4$^+$PD-1$^+$CD45RO$^+$CD45RA$^+$CD4$^+$ transitional memory T cells, the consequence of the downstream signaling events leading to phenotypic changes should be investigated. Also, the limit of the number of naturally occurring CD45RO$^+$CD45RA$^+$CD4$^+$ T cells for studying how Δ42PD1$^+$Vδ2 cells or other APCs can influence them *ex vivo* should also be addressed with a more robust model.

Resource Availability

Lead Contact

Further information and requests for resources and reagents should be directed to and will be fulfilled by the Lead Contact, Allen Ka Loon Cheung (akcheung@hkbu.edu.hk).

Materials Availability

This study did not generate new unique reagents.

Data and Code Availability

This study did not generate any datasets or code.

METHODS

All methods can be found in the accompanying Transparent Methods supplemental file.

SUPPLEMENTAL INFORMATION

Supplemental Information can be found online at https://doi.org/10.1016/j.isci.2020.101620.

ACKNOWLEDGMENTS

We thank Jingjing Li and Dongyan Zhou for generating the anti-Δ42PD1 monoclonal antibodies. This work was supported by Hong Kong Research Grant Council TRS-T11-706/18-N, GRF17115818, GRF17104919, GRF17103514, and HKU5/CRF/13G, University Development Fund of The University of Hong Kong to AIDS Institute and the National Science and Technology Major Project 2018ZX10731-101-002-001 (to Z.C.); and Health and Medical Research Fund (HMRF) (15140732 and 18170032), Interdisciplinary Research Matching Scheme (RC-IRCs-1718-03), Faculty Research Grant (FRG2/17–18/066), Faculty Start-up Fund (SCI-17-18-01), Tier 2 Start-up Grant (RC-SGT2/18–19/SCI/007), and Research Council Start-up Grant of Hong Kong Baptist University (to A.K.L.C.).

AUTHOR CONTRIBUTION

Conceptualization, A.K.L.C. and Z.C.; Methodology, A.K.L.C., Y.M., and Z.C.; Investigation, A.K.L.C., Y.M., and Y.L.; Writing – Original Draft, A.K.L.C., Y.M., and Z.C.; Writing – Review & Editing, A.K.L.C., Y.M., and Z.C.; Funding Acquisition, A.K.L.C. and Z.C.; Supervision, A.K.L.C., L.L., and Z.W.

DECLARATION OF INTERESTS

The antibodies against Δ42PD1 is described in the US patent no. 10,047,137B2 (A.K.L.C. and Z.C.).

Received: March 31, 2020
Revised: July 25, 2020
Accepted: September 22, 2020
Published: October 23, 2020

REFERENCES

Ahn, E., Araki, K., Hashimoto, M., Li, W., Riley, J.L., Cheung, J., Sharpe, A.H., Freeman, G.J., Irving, B.A., and Ahmed, R. (2018). Role of PD-1 during effector CD8 T cell differentiation. Proc. Natl. Acad. Sci. U S A *115*, 4749–4754.

Allie, S.R., Zhang, W., Fuse, S., and Usherwood, E.J. (2011). Programmed death 1 regulates development of central memory CD8 T cells after acute viral infection. J. Immunol. *186*, 6280–6286.

Apetoh, L., Ghiringhelli, F., Tesniere, A., Obeid, M., Ortiz, C., Criollo, A., Mignot, G., Maiuri, M.C., Ullrich, E., Saulnier, P., et al. (2007). Toll-like receptor 4-dependent contribution of the immune system to anticancer chemotherapy and radiotherapy. Nat. Med. *13*, 1050–1059.

Baars, P.A., Maurice, M.M., Rep, M., Hooibrink, B., and Van Lier, R.A. (1995). Heterogeneity of the circulating human CD4+ T cell population. Further evidence that the CD4+CD45RA-CD27- T cell subset contains specialized primed T cells. J. Immunol. *154*, 17–25.

Bank, I., Cohen, L., Mouallem, M., Farfel, Z., Grossman, E., and Ben-Nun, A. (2002). Gammadelta T cell subsets in patients with arthritis and chronic neutropenia. Ann. Rheum. Dis. *61*, 438–443.

Bieback, K., Breer, C., Nanan, R., Ter Meulen, V., and Schneider-Schaulies, S. (2003). Expansion of human gamma/delta T cells in vitro is differentially regulated by the measles virus glycoproteins. J. Gen. Virol. *84*, 1179–1188.

Brandes, M., Willimann, K., Bioley, G., Levy, N., Eberl, M., Luo, M., Tampe, R., Levy, F., Romero, P., and Moser, B. (2009). Cross-presenting human gammadelta T cells induce robust CD8+ alphabeta T cell responses. Proc. Natl. Acad. Sci. U S A *106*, 2307–2312.

Brandes, M., Willimann, K., Lang, A.B., Nam, K.H., Jin, C., Brenner, M.B., Morita, C.T., and Moser, B. (2003). Flexible migration program regulates gamma delta T-cell involvement in humoral immunity. Blood *102*, 3693–3701.

Brandes, M., Willimann, K., and Moser, B. (2005). Professional antigen-presentation function by human gd T cells. Science *309*, 264–268.

Cairns, B., Maile, R., Barnes, C.M., Frelinger, J.A., and Meyer, A.A. (2006). Increased toll-like receptor 4 expression on T cells may Be a mechanism for enhanced T cell response late after burn injury. J. Trauma *61*, 293–299.

Caramalho, I., Lopes-Carvalho, T., Ostler, D., Zelenay, S., Haury, M., and Demengeot, J. (2003). Regulatory T cells selectively express toll-like receptors and are activated by lipopolysaccharide. J. Exp. Med. *197*, 403–411.

Cheung, A.K.L., Kwok, H.Y., Huang, Y., Chen, M., Mo, Y., Wu, X., Lam, K.S., Kong, H.K., Lau, T.C.K., Zhou, J., et al. (2017). Gut-homing Delta42PD1(+) Vdelta2 T cells promote innate mucosal damage via TLR4 during acute HIV type 1 infection. Nat. Microbiol. *2*, 1389–1402.

Cohen-Sfady, M., Nussbaum, G., Pevsner-Fischer, M., Mor, F., Carmi, P., Zanin-Zhorov, A., Lider, O., and Cohen, I.R. (2005). Heat shock protein 60 activates B cells via the TLR4-MyD88 pathway. J. Immunol. *175*, 3594–3602.

Corinti, S., Medaglini, D., Cavani, A., Rescigno, M., Pozzi, G., Ricciardi-Castagnoli, P., and Girolomoni, G. (1999). Human dendritic cells very efficiently present a heterologous antigen expressed on the surface of recombinant gram-positive bacteria to CD4+ T lymphocytes. J. Immunol. *163*, 3029–3036.

Dechanet, J., Merville, P., Lim, A., Retiere, C., Pitard, V., Lafarge, X., Michelson, S., Meric, C., Hallet, M.M., Kourilsky, P., et al. (1999). Implication of gammadelta T cells in the human immune response to cytomegalovirus. J. Clin. Invest. *103*, 1437–1449.

Eberl, M., Hintz, M., Reichenberg, A., Kollas, A.-K., Wiesner, J., and Jomaa, H. (2003). Microbial isoprenoid biosynthesis and human gammadelta T cell activation. FEBS Lett. *544*, 4–10.

Evans, P.S., Enders, P.J., Yin, C., Ruckwardt, T.J., Malkovsky, M., and Pauza, C.D. (2001). In vitro stimulation with a non-peptidic alkylphosphate expands cells expressing Vgamma2-Jgamma1.2/Vdelta2 T-cell receptors. Immunology *104*, 19–27.

Gandhapudi, S.K., Chilton, P.M., and Mitchell, T.C. (2013). TRIF is required for TLR4 mediated adjuvant effects on T cell clonal expansion. PLoS One *8*, e56855.

Girardi, M. (2006). Immunosurveillance and immunoregulation by gammadelta T cells. J. Invest. Dermatol. *126*, 25–31.

Gober, H.-J., Kistowska, M., Angman, L., Jenö, P., Mori, L., and De Libero, G. (2003). Human T cell receptor gammadelta cells recognize endogenous mevalonate metabolites in tumor cells. J. Exp. Med. *197*, 163–168.

González-Navajas, J.M., Fine, S., Law, J., Datta, S.K., Nguyen, K.P., Yu, M., Corr, M., Katakura, K., Eckman, L., Lee, J., and Raz, E. (2010). TLR4 signaling in effector CD4+ T cells regulates TCR activation and experimental colitis in mice. J. Clin. Invest. *120*, 570–581.

Hamann, D., Baars, P.A., Hooibrink, B., and Van Lier, R.W. (1996). Heterogeneity of the human CD4+ T-cell population: two distinct CD4+ T-cell subsets characterized by coexpression of CD45RA and CD45RO isoforms. Blood *88*, 3513–3521.

Harly, C., Guillaume, Y., Nedellec, S., Peigné, C.-M., Mönkkönen, H., Mönkkönen, J., Li, J., Kuball, J., Adams, E.J., Netzer, S., et al. (2012). Key implication of CD277/butyrophilin-3 (BTN3A) in cellular stress sensing by a major human γδ T-cell subset. Blood *120*, 2269–2279.

Himoudi, N., Morgenstern, D.A., Yan, M., Vernay, B., Saraiva, L., Wu, Y., Cohen, C.J., Gustafsson, K., and Anderson, J. (2012). Human gammadelta T lymphocytes are licensed for professional antigen presentation by interaction with opsonized target cells. J. Immunol. *188*, 1708–1716.

Hu, C., Qian, L., Miao, Y., Huang, Q., Miao, P., Wang, P., Yu, Q., Nie, H., Zhang, J., He, D., et al. (2012). Antigen-presenting effects of effector memory Vgamma9Vdelta2 T cells in rheumatoid arthritis. Cell. Mol. Immunol. *9*, 245–254.

Jin, B., Sun, T., Yu, X.-H., Yang, Y.-X., and Yeo, A.E.T. (2012). The effects of TLR activation on T-cell development and differentiation. Clin. Dev. Immunol. *2012*, 836485.

Johannisson, A., and Festin, R. (1995). Phenotype transition of CD4+ T cells from CD45RA to CD45R0 is accompanied by cell activation and proliferation. Cytometry *19*, 343–352.

Kapsenberg, M.L. (2003). Dendritic-cell control of pathogen-driven T-cell polarization. Nat. Rev. Immunol. *3*, 984–993.

Klenerman, P., and Oxenius, A. (2016). T cell responses to cytomegalovirus. Nat. Rev. Immunol. *16*, 367–377.

Komai-Koma, M., Gilchrist, D.S., and Xu, D. (2009). Direct recognition of LPS by human but not murine CD8 +T cells viaTLR4 complex. Eur. J. Immunol. *39*, 1564–1572.

Komai-Koma, M., Jones, L., Ogg, G.S., Xu, D., and Liew, F.Y. (2004). TLR2 is expressed on activated T cells as a costimulatory receptor. PNAS *101*, 3029–3034.

Landmeier, S., Altvater, B., Pscherer, S., Juergens, H., Varnholt, L., Hansmeier, A., Bollard, C.M., Moosmann, A., Bisping, G., and Rossig, C. (2009). Activated human γδ T cells as stimulators of specific CD8+ T-cell responses to subdominant Epstein Barr virus epitopes. J. Immunother. *32*, 310–321.

Mata-Haro, V., Cekic, C., Martin, M., Chilton, P.M., Casella, C.R., and Mitchell, T.C. (2007). The vaccine adjuvant monophosphoryl lipid A as a TRIF-biased agonist of TLR4. Science *316*, 1628–1632.

Meuter, S., Eberl, M., and Moser, B. (2010). Prolonged antigen survival and cytosolic export in cross-presenting human gammadelta T cells. PNAS *107*, 8730–8735.

Mo, W.X., Yin, S.S., Chen, H., Zhou, C., Zhou, J.X., Zhao, L.D., Fei, Y.Y., Yang, H.X., Guo, J.B., Mao, Y.J., et al. (2017). Chemotaxis of Vdelta2 T cells to the joints contributes to the pathogenesis of rheumatoid arthritis. Ann. Rheum. Dis. *76*, 2075–2084.

Moser, B., and Brandes, M. (2006). γδ T cells: an alternative type of professional APC. Trends Immunol. *27*, 112–118.

Moser, B., and Eberl, M. (2007). Gammadelta T cells: novel initiators of adaptive immunity. Immunol. Rev. *215*, 89–102.

Picker, L.J., Treer, J.R., Ferguson-Darnell, B., Collins, P.A., Buck, D., and Terstappen, L.W. (1993). Control of lymphocyte recirculation in man. I. Differential regulation of the peripheral lymph node homing receptor L-selectin on T cells during the virgin to memory cell transition. J. Immunol. *150*, 1105–1121.

Pitard, V., Roumanes, D., Lafarge, X., Couzi, L., Garrigue, I., Lafon, M.E., Merville, P., Moreau, J.F., and Dechanet-Merville, J. (2008). Long-term expansion of effector/memory Vdelta2-gammadelta T cells is a specific blood signature of CMV infection. Blood *112*, 1317–1324.

Rahman, A.H., Taylor, D.K., and Turka, L.A. (2009). The contribution of direct TLR signaling to T cell responses. Immunol. Res. *45*, 25–36.

Rauser, G., Einsele, H., Sinzger, C., Wernet, D., Kuntz, G., Assenmacher, M., Campbell, J.D.M., and Topp, M.S. (2004). Rapid generation of combined CMV-specific CD4+ and CD8+ T-cell lines for adoptive transfer into recipients of allogeneic stem cell transplants. Blood *103*, 3565–3572.

Reynolds, J.M., Martinez, G.J., Chung, Y., and Dong, C. (2012). Toll-like receptor 4 signaling in T cells promotes autoimmune inflammation. PNAS *109*, 13064–13069.

Rigau, M., Ostrouska, S., Fulford, T.S., Johnson, D.N., Woods, K., Ruan, Z., Mcwilliam, H.E.G., Hudson, C., Tutuka, C., Wheatley, A.K., et al. (2020). Butyrophilin 2A1 is essential for phosphoantigen reactivity by gammadelta T cells. Science *367*, eaay5516.

Rodriguez-Jorge, O., Kempis-Calanis, L.A., Abou-Jaoude, W., Gutierrez-Reyna, D.Y., Hernandez, C., Ramirez-Pliego, O., Thomas-Chollier, M., Spicuglia, S., Santana, M.A., and Thieffry, D. (2019). Cooperation between T cell receptor and Toll-like receptor 5 signaling for CD4(+) T cell activation. Sci. Signal. *12*, eaar3641.

Simon, S., and Labarriere, N. (2017). PD-1 expression on tumor-specific T cells: friend or foe for immunotherapy? Oncoimmunology *7*, e1364828.

Summers, K.L., O'donnell, J.L., and Hart, D.N. (1994). Co-expression of the CD45RA and CD45RO antigens on T lymphocytes in chronic arthritis. Clin. Exp. Immunol. *97*, 39–44.

Tanaka, Y., Sano, S., Nieves, E., De Libero, G., Rosa, D., Modlin, R.L., Brenner, M.B., Bloom, B.R., and Morita, C.T. (1994). Nonpeptide ligands for human gamma delta T cells. PNAS *91*, 8175–8179.

Tripathy, A., Khanna, S., Padhan, P., Smita, S., Raghav, S., and Gupta, B. (2017). Direct recognition of LPS drive TLR4 expressing CD8(+) T cell activation in patients with rheumatoid arthritis. Sci. Rep. *7*, 933.

Trushin, S.A., Bren, G.D., and Badley, A.D. (2009). CD4 T cells treated with gp120 acquire a

CD45R0+/CD45RA+ phenotype. Open Virol. J. *3*, 21–25.

Tyler, C.J., Mccarthy, N.E., Lindsay, J.O., Stagg, A.J., Moser, B., and Eberl, M. (2017). Antigen-presenting human gammadelta T cells promote intestinal CD4(+) T cell expression of IL-22 and mucosal release of calprotectin. J. Immunol. *198*, 3417–3425.

Vantourout, P., and Hayday, A. (2013). Six-of-the-best: unique contributions of γδ T cells to immunology. Nat. Rev. Immunol. *13*, 88–100.

Vavassori, S., Kumar, A., Wan, G.S., Ramanjaneyulu, G.S., Cavallari, M., El Daker, S., Beddoe, T., Theodossis, A., Williams, N.K., Gostick, E., et al. (2013). Butyrophilin 3A1 binds phosphorylated antigens and stimulates human γδ T cells. Nat. Immunol. *14*, 908–916.

Yang, H., Hreggvidsdottir, H.S., Palmblad, K., Wang, H., Ochani, M., Li, J., Lu, B., Chavan, S., Rosas-Ballina, M., Al-Abed, Y., et al. (2010). A critical cysteine is required for HMGB1 binding to Toll-like receptor 4 and activation of macrophage cytokine release. PNAS *107*, 11942–11947.

Zanin-Zhorov, A., and Cohen, I.R. (2013). Signaling via TLR2 and TLR4 directly down-regulates T cell effector functions: the regulatory face of danger signals. Front. Immunol. *4*, 211.

Zanin-Zhorov, A., Tal-Lapidot, G., Cahalon, L., Cohen-Sfady, M., Pevsner-Fischer, M., Lider, O., and Cohen, I.R. (2007). Cutting edge: T cells respond to lipopolysaccharide innately via TLR4 signaling. J. Immunol. *179*, 41–44.

Zanoni, I., Ostuni, R., Marek, L.R., Barresi, S., Barbalat, R., Barton, G.M., Granucci, F., and Kagan, J.C. (2011). CD14 controls the LPS-induced endocytosis of Toll-like receptor 4. Cell *147*, 868–880.

Zhou, J., Cheung, A.K., Liu, H., Tan, Z., Tang, X., Kang, Y., Du, Y., Wang, H., Liu, L., and Chen, Z. (2013). Potentiating functional antigen-specific $CD8^+$ T cell immunity by a novel PD1 isoform-based fusion DNA vaccine. Mol. Ther. *21*, 1445–1455.

Zou, W., and Chen, L. (2008). Inhibitory B7-family molecules in the tumour microenvironment. Nat. Rev. Immunol. *8*, 467–477.

iScience, Volume *23*

Supplemental Information

Δ42PD1-TLR4 Augments γδ-T Cell Activation of the Transitional Memory Subset of $CD4^+$ T Cells

Yufei Mo, Allen Ka Loon Cheung, Yue Liu, Li Liu, and Zhiwei Chen

Supplemental Information

List of Supplemental Figures

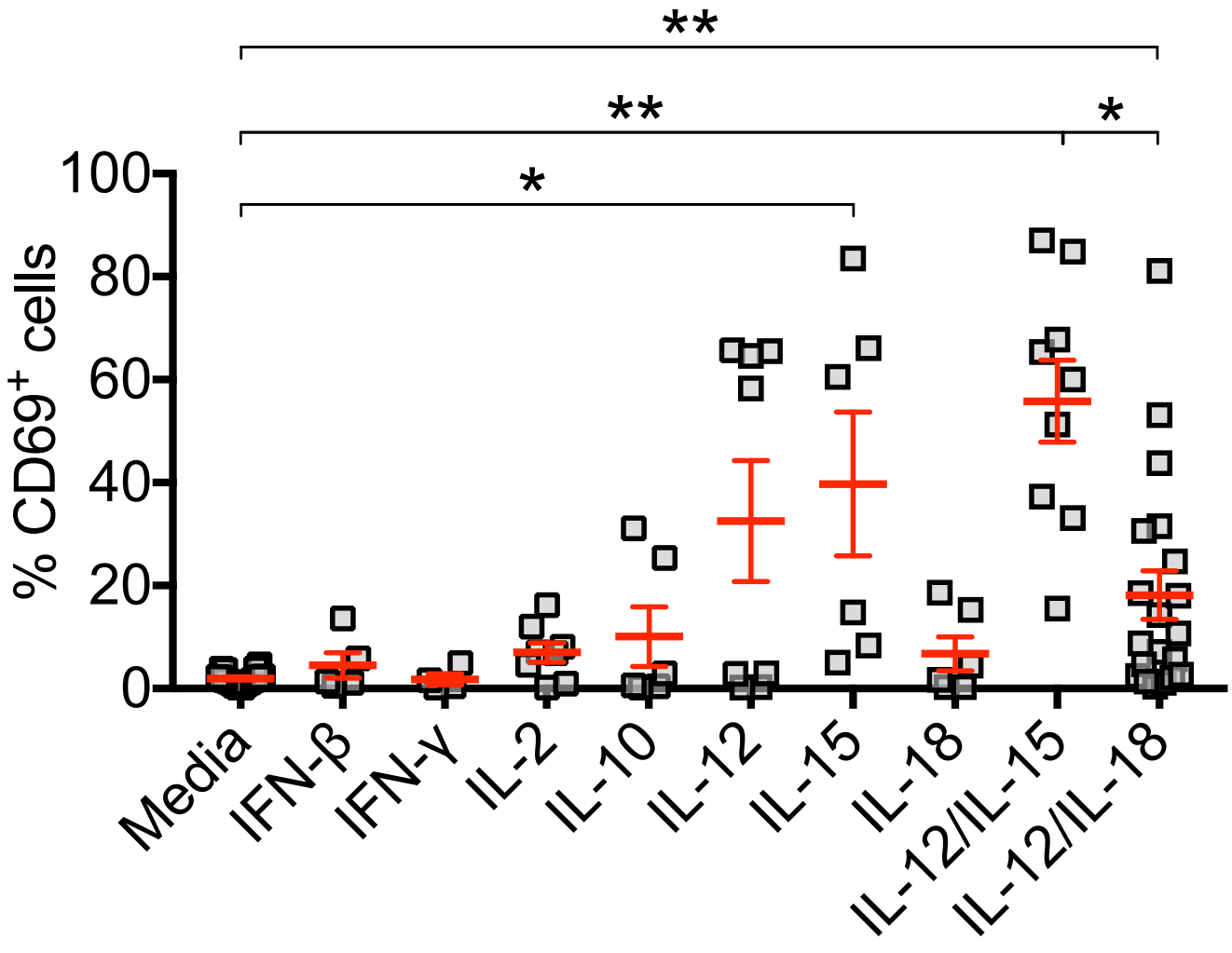

Figure S1. CD69 expression on CD3$^+$Vδ2$^+$ cells by cytokine induction, Related to Figure 1. Purified $\gamma\delta$-T cells from healthy PBMCs were isolated and stimulated with different cytokines for 5 days and analyzed for expression of CD69 by flow cytometry. Data from n≥4 independent experiments are shown as mean±SEM. *P<0.05, **P<0.01.

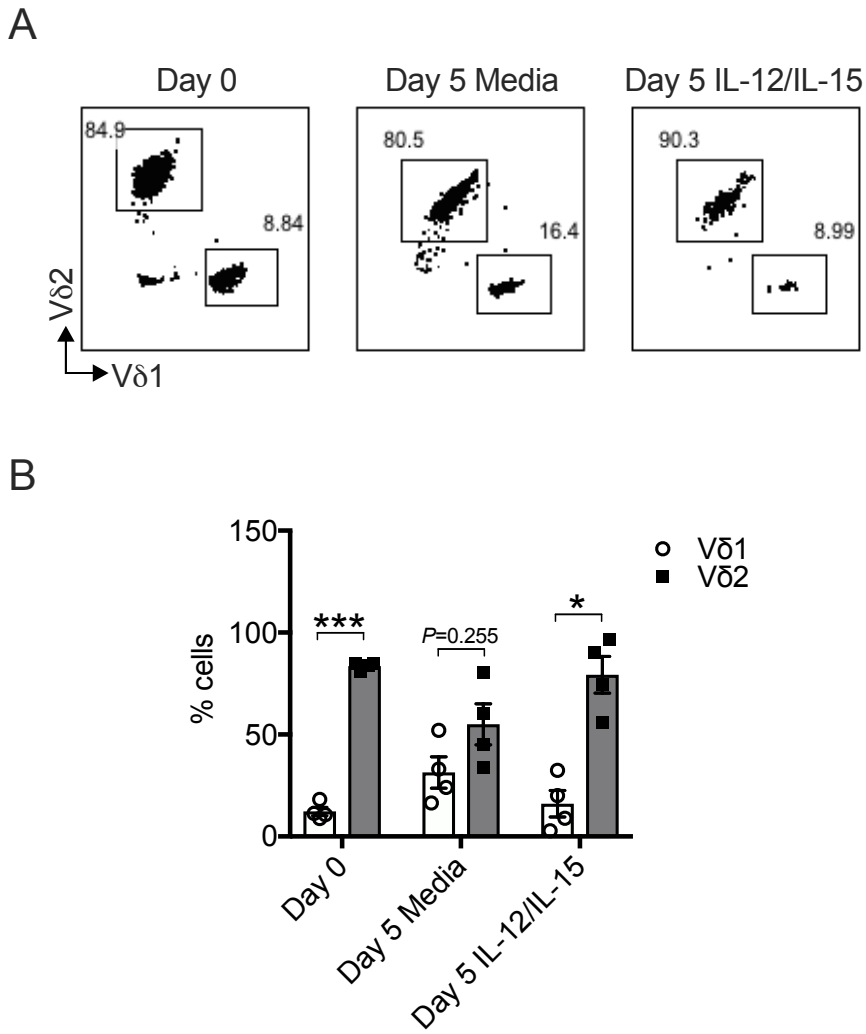

Figure S2. Proportion of Vδ1 and Vδ2 cells following IL-12/IL-15 stimulation, Related to Figure 1. γδ-T cells freshly isolated from PBMCs, treated with IL-12 (4 ng/ml) and IL-15 (20 ng/ml) or left in media for 5 days, were subjected to flow cytometry analysis for Vδ1 and Vδ2 subsets following CD3-gating. (**A**) Representive dot plots. (**B**) Column graph of n=4 independent experiments showing mean±SEM. **P*<0.05, ****P*<0.001.

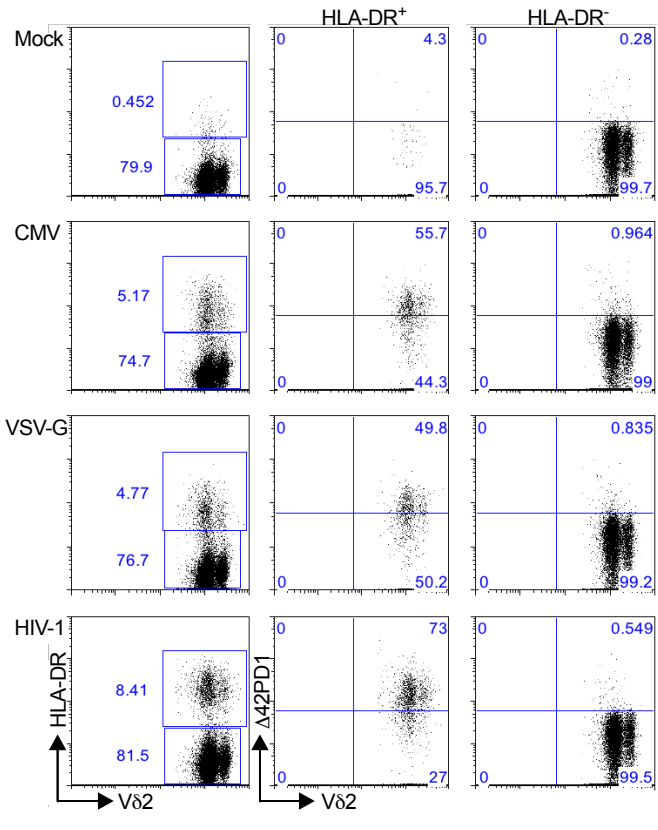

Figure S3. Viral infection induces Δ42PD1 and MHC-II co-expression on Vδ2$^+$ cells, Related to Figure 1. Flow cytometric analysis of the expression of Δ42PD1 and HLA-DR on CD3$^+$Vδ2$^+$ cells after virus infection of PBMCs at day 3 P.I. shown as representative dot plots.

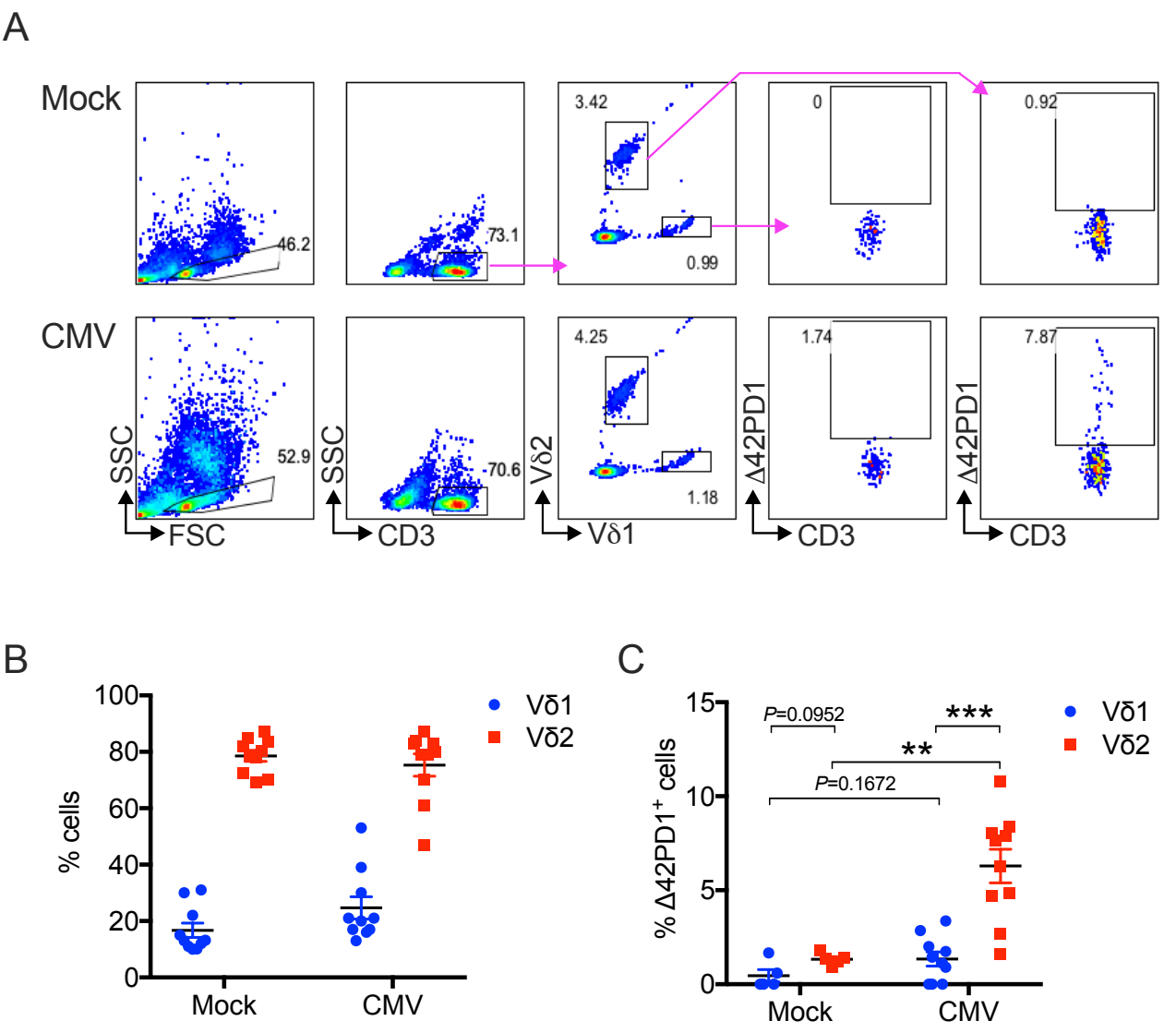

Figure S4. CMV infection of PBMCs did not induce Vδ1 cells, Related to Figure 1. PBMCs were mock or infected with CMV, and assessed by flow cytometry for Vδ1 and Vδ2 subsets and Δ42PD1 expression among $CD3^+$ cells. (**A**) Representive dot plots showing gating strategy. (**B**) Graph of n=10 independent experiments showing mean±SEM. $^{**}P<0.01$, $^{***}P<0.001$.

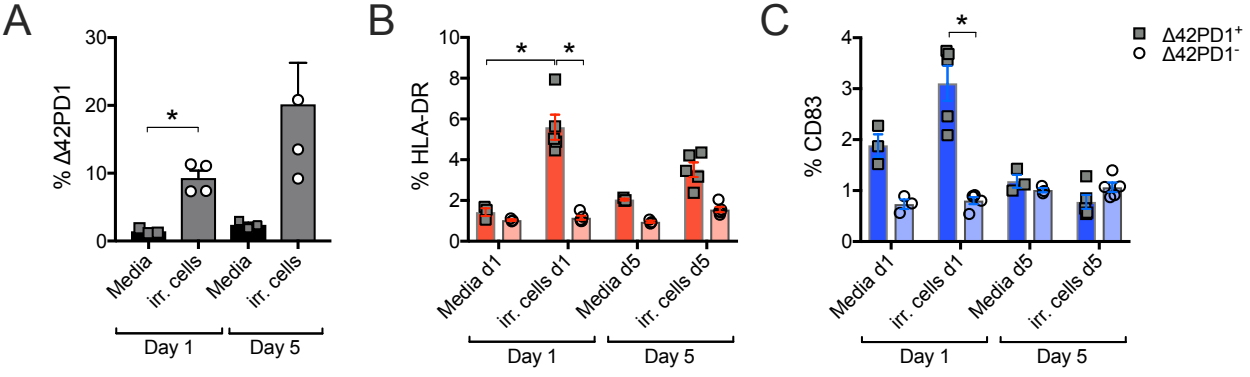

Figure S5. Vδ2 cells respond to irradiated PBMCs by upregulating Δ42PD1, HLA-DR and CD83, Related to Figure 2. Purified γδ-T cells were stimulated with allogeneic irradiated PBMCs and performed flow cytometry analysis gated on $CD3^{+}V\delta2^{+}$ cells for (**A**) Δ42PD1, (**B**) HLA-DR, and (**C**) CD83 expression. (**B, C**) were analyzed on $\Delta42PD1^{+}$ and $\Delta42PD1^{-}$ subsets. Data represents mean±SEM from 4 independent experiments. *P<0.05.

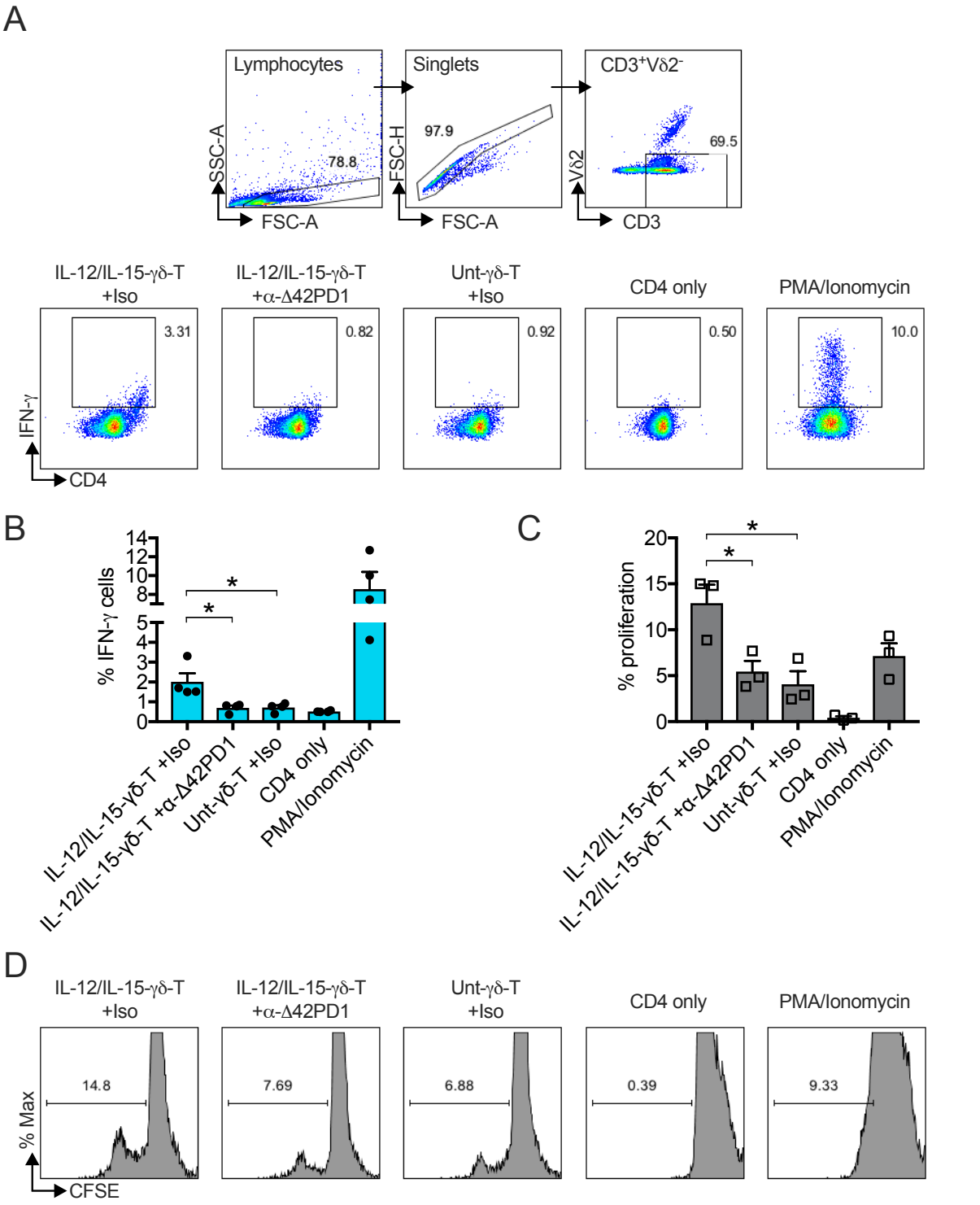

Figure S6. Δ42PD1-TLR4 plays a role in the stimulation of autologous CD4$^+$ T cells, Related to Figure 2. γδ-T cells were isolated from PBMCs and stimulated with IL-12/IL-15 for 5 days before total CD4+ T cells were used for co-culture at a ratio of 1:1 using AIM-V serum-free media and assessed by intracellular IFN-γ detection (n=4) (**A, B**) and CFSE proliferation assays (n=3) (**C, D**). (**A**) Representative dot plots and gating strategies to detect IFN-γ and displayed as a column graph (**B**). (**D**) Representative CFSE proliferation histograms or as a column graph (**C**). Data shows mean±SEM. *P<0.05.

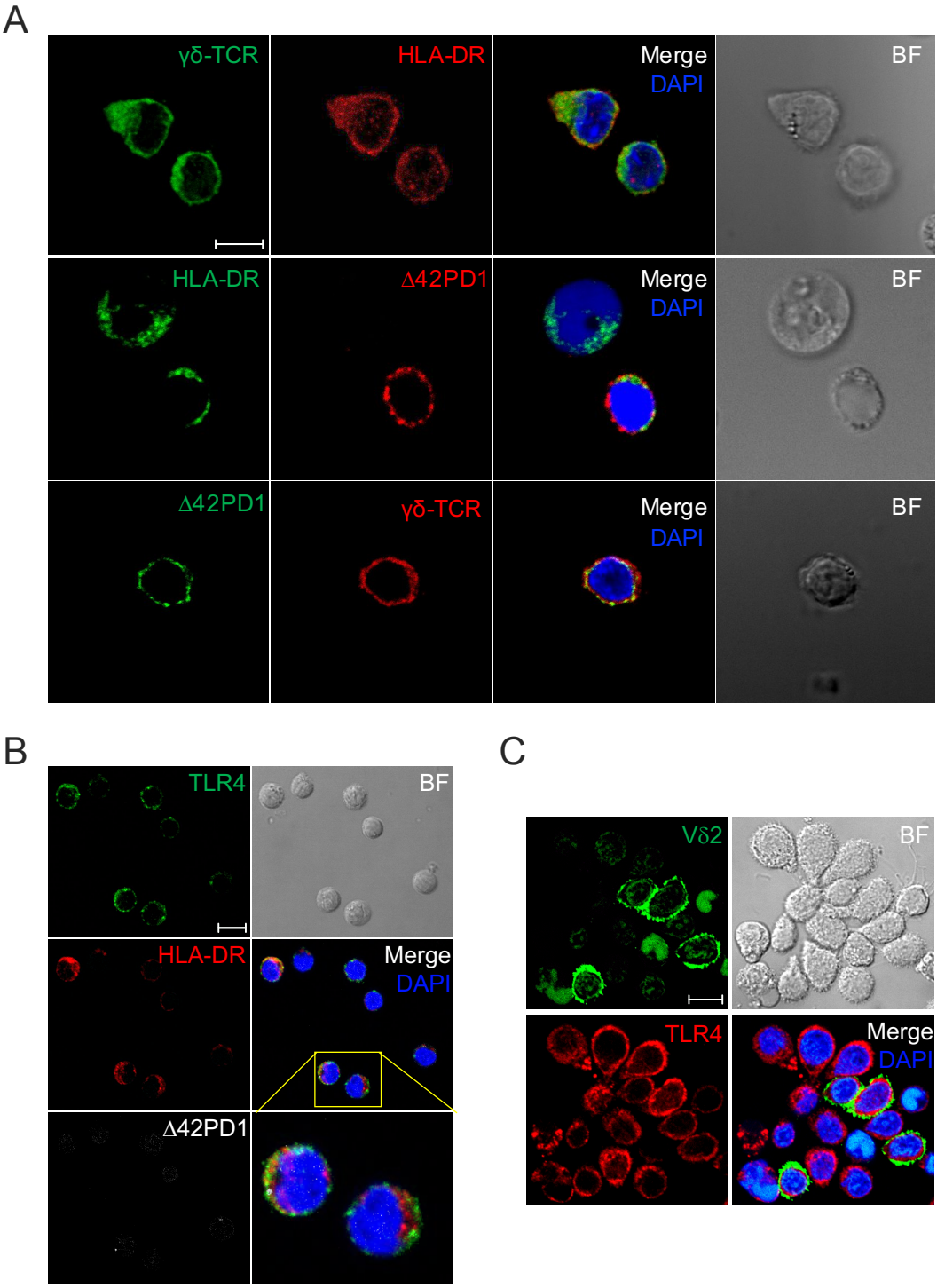

Figure S7. Analysis of Δ42PD1, MHC-II and TLR4 expression on γδ-T cells and CD4$^+$ T cells with confocal microscopy, Related to Figure 3. (A) Purified γδ-T cells were treated with IL-12/IL-15 cytokines for 5 days before immunostained for γδ-TCR, HLA-DR and Δ42PD1 with nuclear stain DAPI. Magnification at 630X. (**B**) pp65-specific CD4$^+$ T cells were immunostained with antibodies against TLR4, HLA-DR and Δ42PD1, then fixed and permeabilized for DAPI staining before spotted onto glass microscope slides for image acquisition. Inset was magnified to the bottom right panel. (**C**) Co-culture of pp65-pulsed Vδ2 cells with pp65-specific TLR4$^+$CD4$^+$ T cells showing cell cluster and interactions. Representative images from three independent experiments are shown. White bar represents a scale of 10 μm.

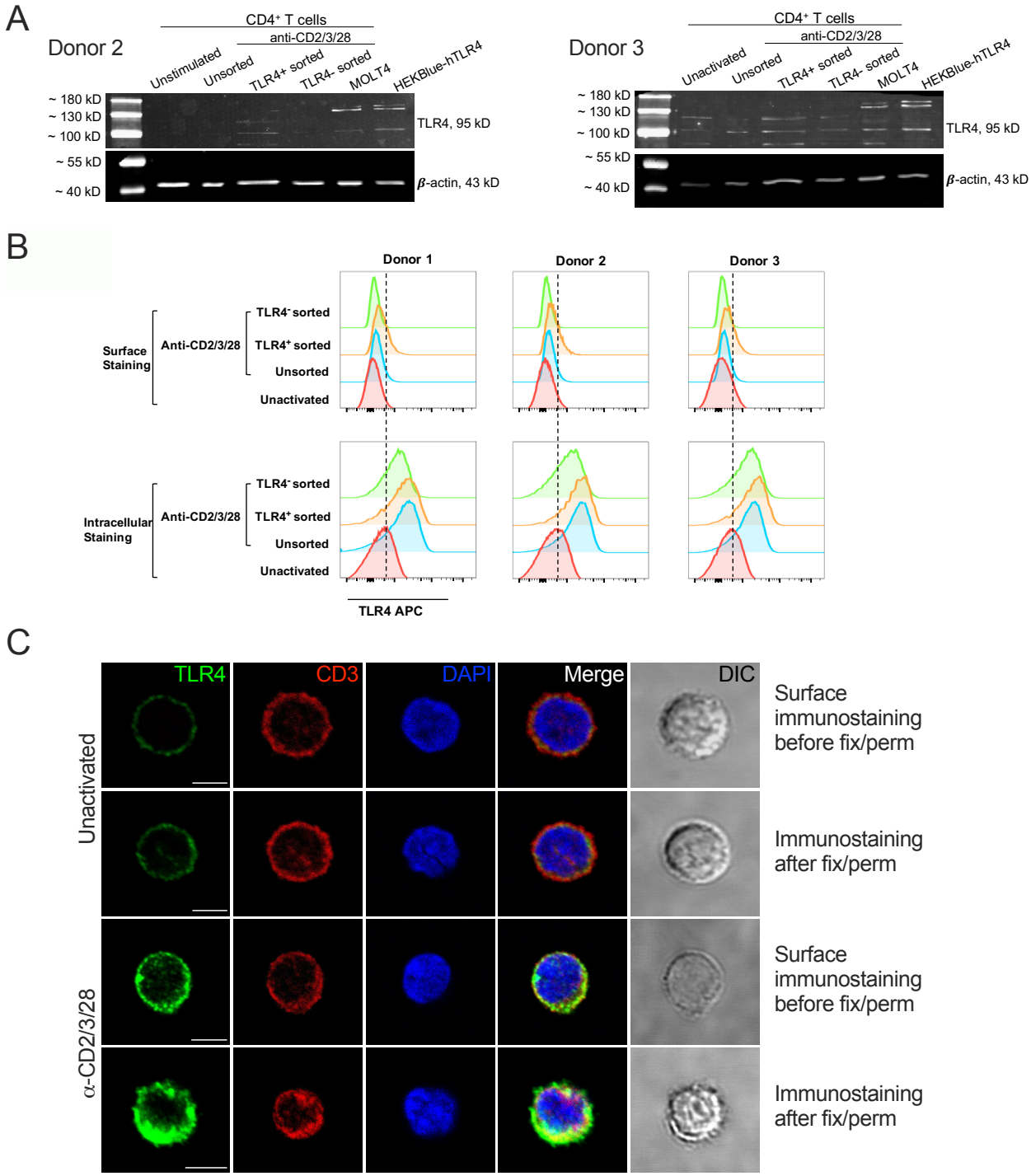

Figure S8. Confirmation of TLR4 expression in CD4$^+$ T cells, Related to Figure 4. Total CD4$^+$ T cells were unactivated or stimulated with anti-CD2/3/28 antibodies for 3 days for 3 independent donors. The stimulated cells were subjected to FACSorting for surface expressed TLR4$^+$ and TLR4$^-$ subpopulations and further assessed. (**A**) Western blotting analysis of CD4$^+$ T cells with MOLT4 and HEKBlue-hTLR4 controls for two independent donors. The donor 1 blot is shown in Figure 4. (**B**) Surface and intracellular flow cytometry to detect TLR4 following FACSorting. TLR4$^+$ sorted cells showed higher TLR4 expression compared to TLR4$^-$ cells. (**C**) Confocal microscopy to assess TLR4 expression on unstimulated or anti-CD2/3/28 treated cells under two experimental protocols of immunostaining with antibodies before or after fix/perm procedure. Increase in surface and cytoplasmic TLR4 expression can be observed. Cells representative of 3 independent donors and from at least 6 images from each treatment are shown. White bar represents a scale of 5 μm.

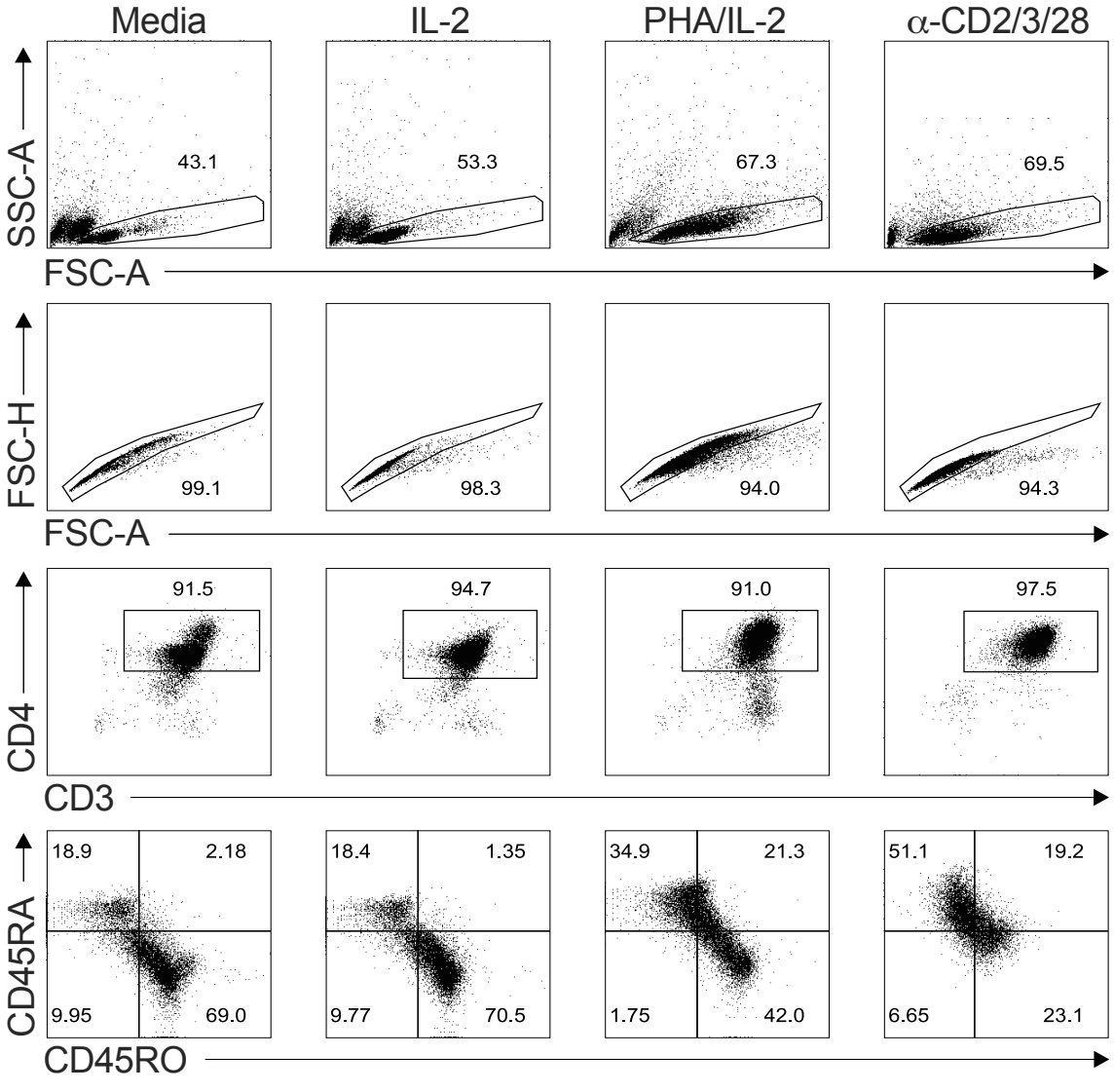

Figure S9. Gating and analysis of unstimulated and stimulated CD4$^+$ T cells that co-expresses CD45RO and CD45RA, Related to Figure 5. PBMCs were left in media or stimulated with IL-2, PHA/IL-2, or anti-CD2/3/28 antibodies for 3 days before analyzed by flow cytometry.

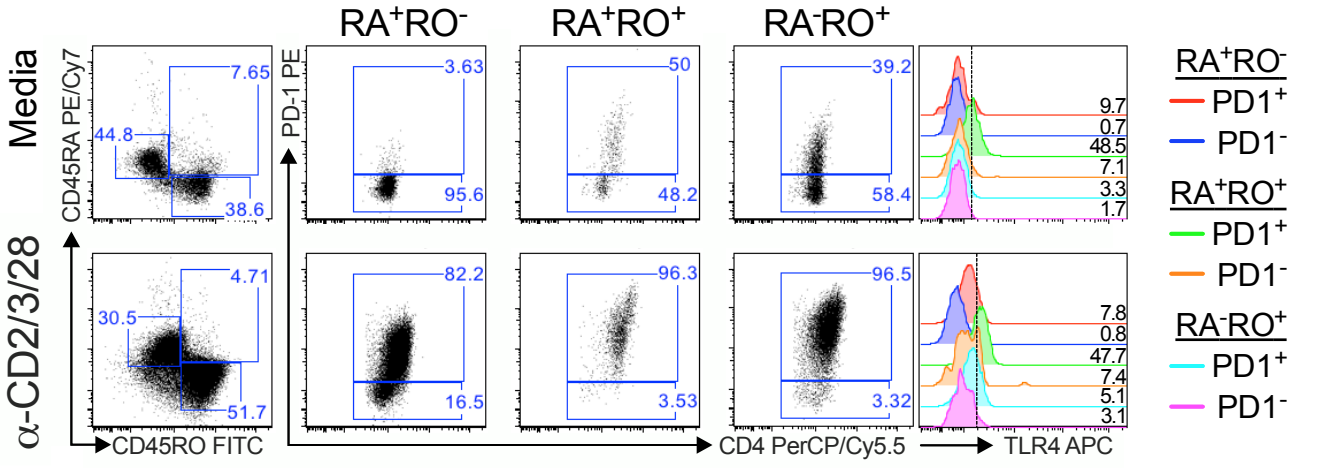

Figure S10. Gating and analysis of TLR4 expression on CD4$^+$ T cell subsets, Related to Figure 5. PBMCs were treated with media or anti-CD2/3/28 antibodies for 3 days before assessed for TLR4 expression on different CD45RA, CD45RO and PD-1 subsets by flow cytometry. Representative dot plots, and histogram plotting %max vs TLR4 expression are shown.

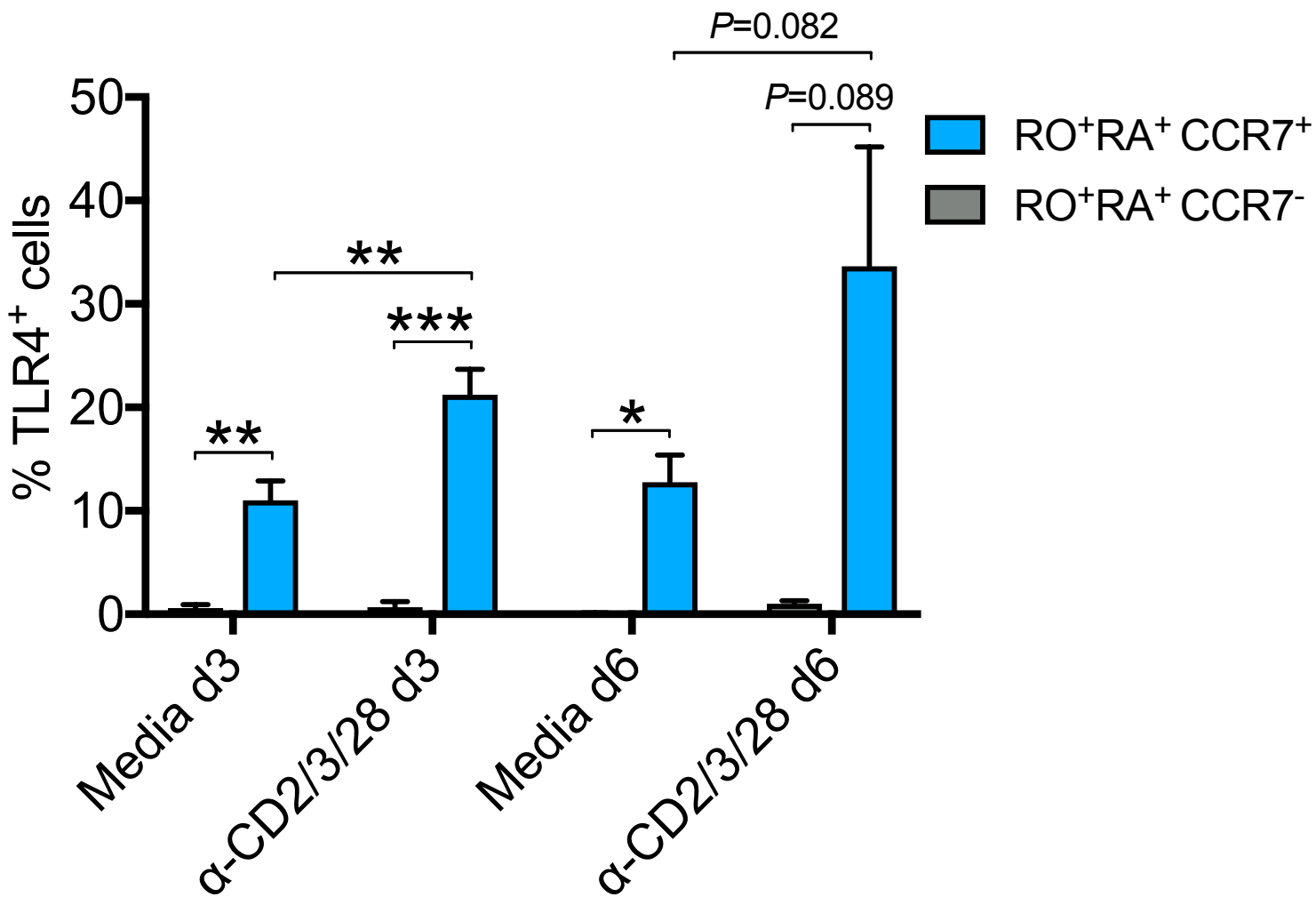

Figure S11. Analysis of TLR4 expression on CCR7$^{+/-}$ CD4^{+} T cell subsets, Related to Figure 5. PBMCs treated with media or anti-CD2/3/28 antibodies for 3 or 6 days before assessed for TLR4 expression on CD45RA^{+}CD45RO^{+} and CCR7$^{+/-}$ subsets by flow cytometry. Graph of data representing mean±SEM from 6 independent experiments. *P<0.05, ***P<0.01, **P<0.001.

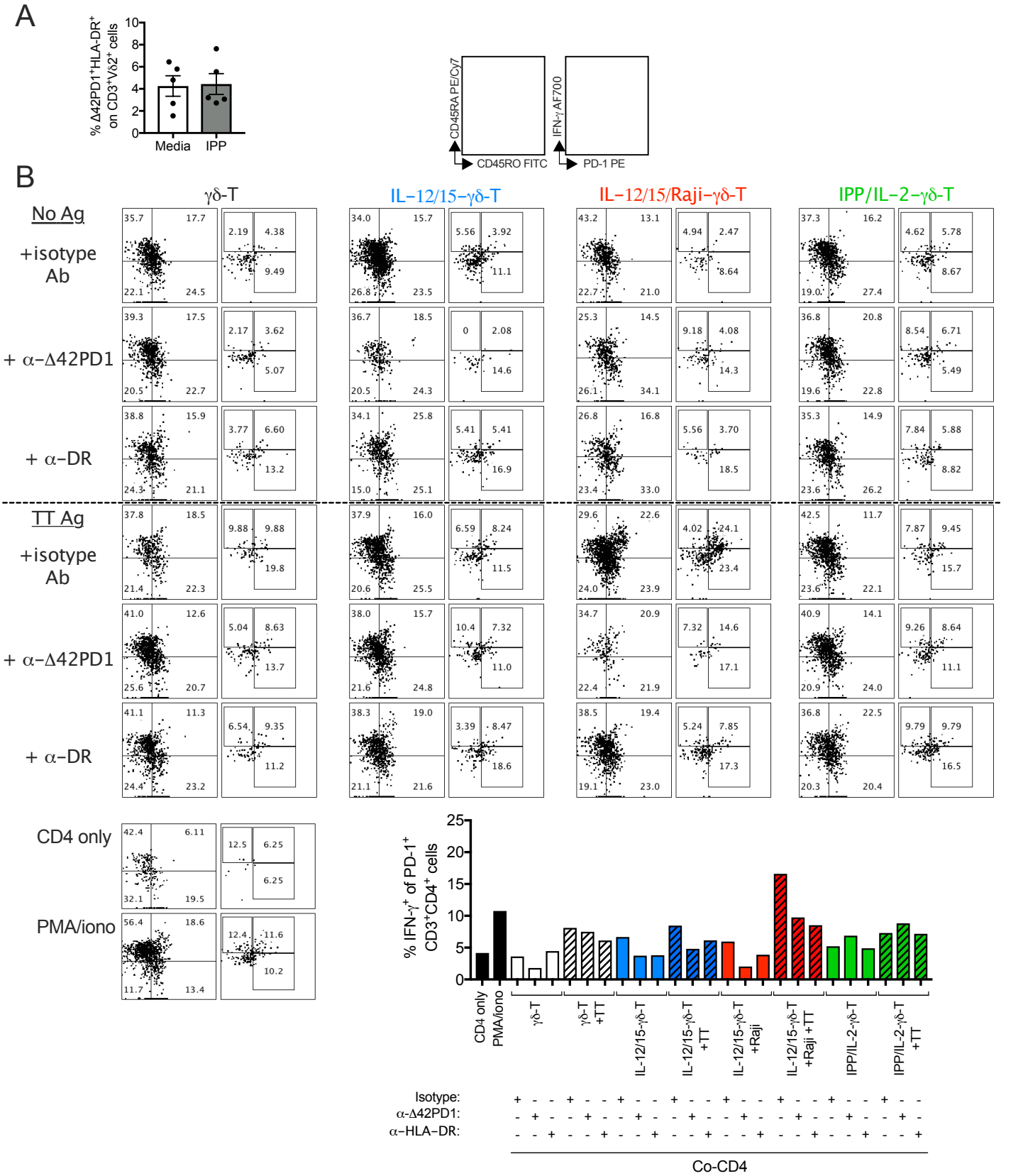

Figure S12. Gating and analysis for TT co-culture experiments, Related to Figure 5. Purified CD4$^+$ T cells were pulsed with TT C-fragment in the presence of irradiated PBMCs to induce TT-specific CD4$^+$ T cells and then total CD4$^+$ T cells was isolated and co-cultured with unstimulated, IL-12/IL-15- or IPP/IL-2 stimulated and/or TT-pulsed γδ-T cells in the presence or absence of Raji feeder cells. Blocking antibodies anti-Δ42PD1 and anti-HLA-DR were used. CD4 only, negative control; CD4 treated with PMA/ionomycin, positive control. Flow cytometry was used to assess intracellular IFN-γ expression in CD45RO and CD45RA subsets. (**A**) IPP/IL-2 was unable to induce Δ42PD1/HLA-DR expression. (**B**) Representative dot plots showing the gating strategy. Mean of two donor samples are plotted as a column graph.

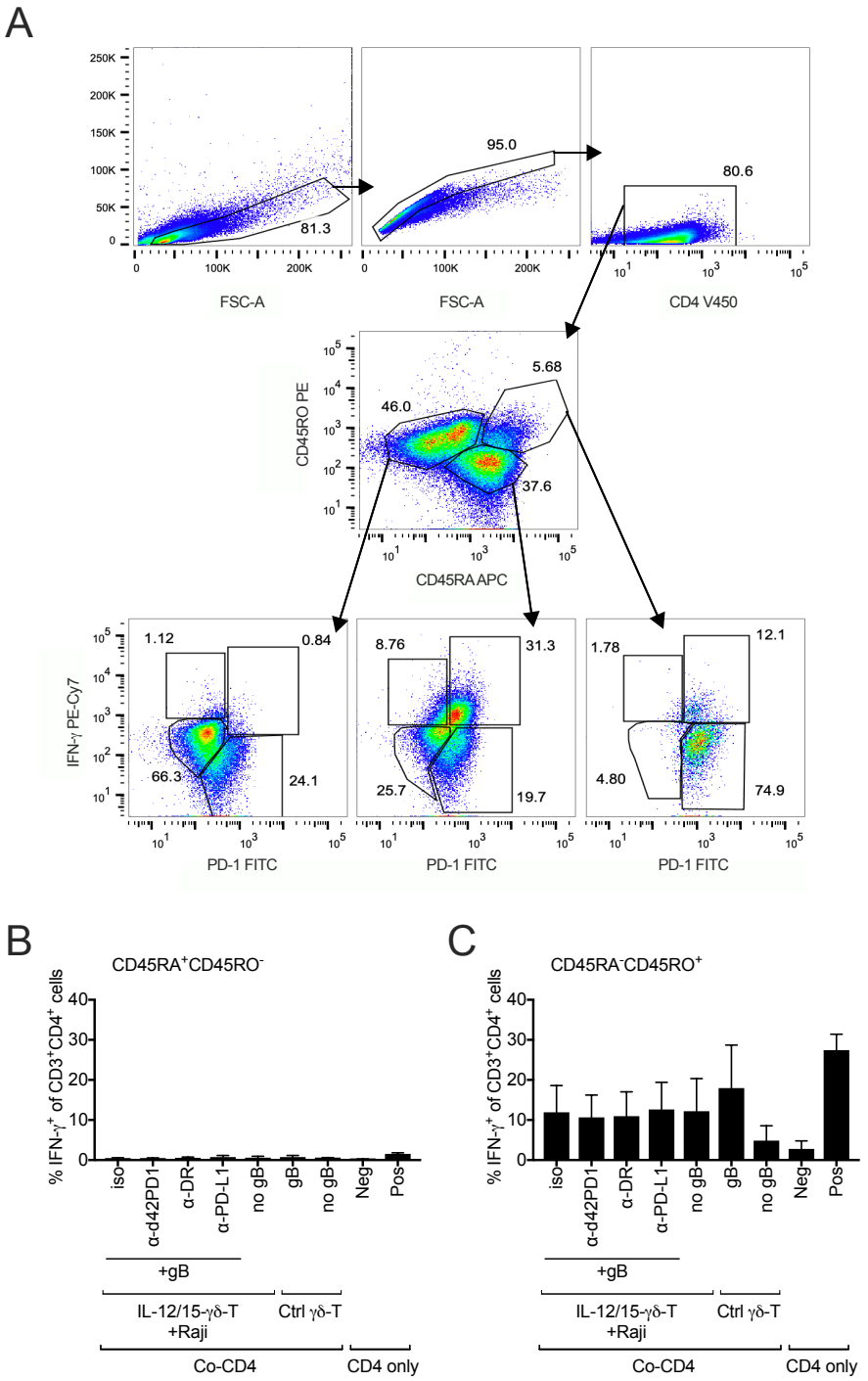

Figure S13. Representative gating and analysis for pp65/gB co-culture experiments, Related to Figure 5. pp65 peptide mix was used to treat PBMCs before $CD4^+$ T cells was isolated and co-cultured with IL-12/IL-15 stimulated and pp65-pulsed purified γδ-T cells in the presence of Raji feeder cells. Blocking antibodies anti-Δ42PD1, anti-HLA-DR and anti-PD-L1 were used. CD4 only, negative control; CD4 treated with PMA/ionomycin, positive control. Flow cytometry was used to assess intracellular IFN-γ expression in CD45RO and CD45RA subsets. Other treatments were analyzed in the same manner. (A) Representative dot plots showing the gating strategy. (B,C) Analysis of the responses of the $CD45RA^+CD45RO^-$ and $CD45RA^-CD45RO^+$ subsets. Pos, PMA/ionomycin. Neg, CD4 cells only. Data plotted as column graphs and represent mean±SEM from 4 independent experiments.

Supplemental Videos (Video S1 to S3 are provided as separate files)

Video S1. Z-stack of pp65-γδ-T cells co-cultured with pp65-specific TLR4$^+$CD4$^+$ T cells, Related to Figure 3. 78 images at 0.29 μm thickness each are presented as a video to show the interaction between pp65-specific CD4$^+$ T cell and pp65-pulsed γδ-T cells. Pixel size = 80.2 nm. Green = TLR4, Red = HLA-DR, White = Δ42PD1, Blue = DAPI.

Video S2. Z-stack of pp65-γδ-T cells co-cultured with pp65-specific TLR4$^+$CD4$^+$ T cells, Related to Figure 3. 78 images at 0.29 μm thickness each are presented as a video to show the interaction between pp65-specific CD4$^+$ T cell and pp65-pulsed γδ-T cells at their individual channels. Pixel size = 80.2 nm. Green = TLR4, Red = HLA-DR, White = Δ42PD1, Blue = DAPI.

Video S3. Imaris analyzed representation of the interaction between pp65-γδ-T cells and pp65-specific TLR4$^+$CD4$^+$ T cells, Related to Figure 3. 25 images each with a thickness of 0.506 μm were used to generate the 3D model. Pixel size = 112 nm. Green = TLR4, Red = HLA-DR, White = Δ42PD1, Blue = DAPI.

Transparent Methods

Cells isolation

Fresh peripheral blood mononuclear cells (PBMCs) were generated following gradient centrifugation using Ficoll-Paque (GE Healthcare) of healthy human blood donor buffy coats. Use of buffy coats received ethics approval from Institutional Review Board of the University of Hong Kong/Hospital Authority Hong Kong West Cluster #UW13-476 and non-clinical human research ethics HASC/17-18/0795 from Hong Kong Baptist University Research Ethics Committee. Monocyte-derived dendritic cells (MoDCs) were generated by 7-day culture of freshly purified CD14$^+$ cells from healthy human PBMCs using positive selection CD14 microbeads (>95% purity; Miltenyi Biotec) in RPMI 1640 medium supplemented with 10% fetal bovine serum (FBS; GIBCO), 2 mM L-glutamine (GIBCO), 100 U/ml penicillin /100 μg/ml streptomycin (GIBCO), 10 mM HEPES (GIBCO), 2 mM β-mercaptoethanol (GIBCO), 50 ng/ml each of recombinant human GM-CSF and IL-4 (Miltenyi Biotec). 50% media change occurred every 3 days. γδ-T cells were isolated from fresh PBMCs using γδ-T cell isolation kit (>95% purity, Miltenyi Biotec) by negative selection to avoid unnecessary activation.

Proportion of Vδ1/Vδ2 cells were assessed by flow cytometry. Total $CD4^+$ T cells or naïve $CD4^+$ T cells were purified from frozen or fresh PBMCs using respective microbeads by negative selection (>95% purity, Miltenyi Biotec).

Cytokine and phosphoantigen activation of γδ-T cells

Purified γδ-T cells were treated with the following cytokines: IFN-β (0.2 μg/ml, PeproTech), IFN-γ (20 ng/ml, PeproTech) or, IL-2 (40 U/ml, R&D Systems), IL-10 (20 ng/ml, PeproTech), IL-12 (4 ng/ml, Miltenyi Biotec), IL-15 (20 ng/ml, Miltenyi Biotec), IL-18 (20 ng/ml, R&D Systems), IL-12/IL-15 and IL-12/IL-18. Isopentenyl pyrophosphate (IPP; Sigma-Aldrich) at 50 μM was used for activation. At least 2×10^5 cells were used per well in a 96-well plate with 0.2 ml volume. After 5 days of treatment, cells were assessed by flow cytometry.

$CD4^+$ T cell activation

Purified $CD4^+$ T cells were activated by phytohaemagglutinin (PHA, 5 μg/ml, Sigma-Aldrich) plus IL-2 (40 U/ml, R&D Systems), or phorbol 12-myristate-13-acetate (PMA, 400 ng/mL, Sigma-Aldrich) plus ionomycin (1000 ng/mL, Sigma-Aldrich) or anti-CD2/3/28 antibodies (Human T Cell Activation/Expansion Kit, Miltenyi Biotec), serving as a treatment for CD4 T cells or a positive control for co-culture experiments.

Viruses

Human cytomegalovirus strain AD169 (CMV) was propagated in MRC-5 cells (ATCC) and cell-free virus was prepared to infect cells at a multiplicity of infection (MOI)=0.1 for 3 h at 1 x 10^6 cells per ml RPMI 1640/10% FBS as described previously (Cheung et al., 2006). HIV-1 NL4-3 (HIV-1) or pseudotyped with vesicular stomatitis virus glycoprotein (VSV-G) was

prepared and used for infection as previously described (Kang et al., 2012). Flow cytometry was performed to assess HLA-DR and Δ42PD1 expression (see below).

Western blotting

Cells were lysed with a denaturing lysis buffer (10 mM Tris-HCL (pH 7.5), 200 mM NaCl, 1 mM EDTA, 1 mM DTT, 0.5% NP-40, 1 mM PMSF, 10 μg/ml aprotinin, 10 μg/ml leupeptin, 1.25 μg/ml pepstatin A). For western blotting, protein samples (50 μg) were boiled for 5 min before loaded onto 4-12% SDS-PAGE gel for electrophoresis and transferred to PVDF membrane (Millipore) using a Mini Trans-Blot® Wet/Tank Blotting Systems (Bio-Rad). Membrane was blocked using PBS-T with 0.5% bovine serum albumin (BSA) and 5% Blotting-Grade Blocker (Bio-Rad) for 1 h, before incubated with primary antibodies against TLR4 (clone 25, Santa Cruz) or β-actin (clone AC-15, Abcam) for 8-16 h. For ECL Western blotting, the blot was incubated with HRP-conjugated secondary antibodies anti-mouse IgG HRP and anti-rabbit IgG HRP (GE Healthcare), and the blot was later developed using SuperSignal West Femto Maximum Sensitivity Substrate (Thermo Fisher Scientific) for TLR4, and Pierce™ ECL Western Blotting Substrate was used for developing β-actin signal, captured by Amersham Hyperfilm ECL (GE Healthcare).

Antibodies for flow cytometry

For flow cytometry, the following antibodies against human surface proteins were used: anti-CD3 Pacific Blue (PB; clone UCHT1, BD Biosciences #558117), anti-CD3 PE (clone HIT3a, Biolegend), anti-Vδ1 FITC (clone REA173, Miltenyi Biotec #130-100-532) and anti-Vδ2 PE (clone B6, BD Biosciences #555739), anti-CD4 PerCP-Cy5.5 (clone OKT4, Biolegend #317428), anti-CD4 FITC (clone OKT4, Biolegend #317408), anti-CD4 V450 (clone RPA-T4, BD Horizon #561838) anti-CD11c PE (clone 3.9, Biolegend #301606), anti-CD14

PerCP/Cy5.5 (eBioscience #45-0149-42), anti-CD45RA PE/Cy7 (clone HI100, Biolegend #304126), anti-CD45RA APC (REA562, Miltenyi Biotec #130-113-362), anti-CD45RO FITC (clone UCHL1, BD Science #555492), anti-CD45RO PE (clone UCHL1, BD Pharmingen #561889), anti-CCR7 PE (clone G043H7, Biolegend #353204), anti-CD69 APC/Cy7 (clone FN50, Biolegend #310914), anti-CD83 (clone HB15e, BD Sciences #562631), anti-HLA-DR PE/Cy7 (clone LN3, eBioscience #25-9956-42), anti-PD-1 PE (clone EH12.2H7, Biolegend #329906), anti-PD-1 FITC (clone MIH4, BD Pharmingen #557860), and anti-TLR4 APC (clone HTA125, eBiosciences #17-9917-42). These antibodies were used for intracellular staining: anti-IFN-γ AF700 (clone B27, Biolegend #506516), anti-IFN-γ FITC (clone 4S.B3, BD Biosciences #554551), and anti-IFN-γ PE-Cy7 (clone 4S.B3, BD Pharmingen #560741). Relevant matching isotype controls were used. A mouse monoclonal (m)Ab against Δ42PD1 (Clone CH101) was generated and used as we previously described (Cheng et al., 2015, Cheung et al., 2017).

Analysis of TLR4 expression in FACSorted CD4$^+$ T cells

Primary CD4$^+$ T cells were purified from PBMCs by negative selection (Miltenyi Biotec kit) and activated by anti-CD2/3/28 antibodies (Miltenyi Biotec) for 3 days. TLR4$^+$ and TLR4$^-$ subsets were sorted from anti-CD2/3/28 stimulated CD4$^+$ T cells using BD Aria III instrument. MOLT4 cells were used for negative control and HEKBlue-hTLR4 cells (Invivogen) served as positive control. Total protein harvested from cell lysates were used for Western blotting assay with primary antibodies against TLR4 and β-actin and with secondary antibodies conjugated to fluorescent dye (IRDye 680RD, LI-COR) for quantification purpose. Sapphire Biomolecular Imager (Azure Biosystems) were used for fluorescent signal detection with intensity level at 5 for TLR4 and at 2 for β-actin control. Although MOLT4 cells was used as negative control but still showed a weak signal, different from the data from the Human Protein Atlas website

(https://www.proteinatlas.org). Band intensities were measured using ImageJ to calculate normalized TLR4 signals against β-actin.

Immunofluorescence confocal microscopy

Purified γδ-T cells were seeded on µ-plate 96-well black (#89626, ibidi) and treated with IL-12 (4 ng/ml) together with IL-15 (20 ng/ml) for 5 days at 37°C with 5% CO_2, before cells were fixed and immunostained with anti-γδ-TCR (clone 5A6.E9 or clone γ3.20, Thermo Fisher Scientific), anti-Vδ2 (clone 15D, Thermo Fisher Scientific), anti-HLA-DR3 (clone L243, Novus Biologicals #NB100-77855) and anti-Δ42PD1 (clone CH34) antibodies and analyzed by Carl Zeiss LSM 700 confocal microscope.

Co-culture of γδ-T cells and CD4 T cells were performed in the Nunc™ Lab-Tek™ II 8-well chambered coverglass (#Z734853, Thermo Fischer Scientific), before fixed and immunostained using primary antibodies against HLA-DR3 (clone L243, Novus Biologicals), Δ42PD1 (CH34), TLR4 (clone 25 or HTA125, Santa Cruz), and appropriate secondary antibodies conjugated with AlexaFluor 488, 568, or 647. All cells were mounted using SlowFade Gold antifade reagent with DAPI (Invitrogen). Signals were acquired using Carl Zeiss LSM700, LSM800 or Leica SP5 II confocal microscopes and images were analyzed using ZEN (Blue), ZEN (Black), and ImageJ software (http://imagej.nih.gov/ij/) (Schneider et al., 2012). Z-stacks between co-culture of γδ-T cells and $CD4^+$ T cells were generated at a thickness of 0.26 µm. Cell-cell interactions and signals between Δ42PD1, HLA-DR, and TLR4 were performed on individual images of one Z-plane across a given line indicated in the image in Figure 3D. Up to 32 cell-cell pairs were analyzed and the intensity values across a distance of 20 pixels from -10 to 10, where the interacting point is set at 0, were used for means and presented as a line graph. Co-localization coefficients for Overlap and Manders' were calculated using the JACoP plug-in in ImageJ after setting the appropriate threshold to remove

noise (Costes et al., 2004). Imaris software (v7.5.2, Oxford Instruments) was used to generate 3D models and animations based on the fluorescence Z-stack maximum projection images of 25 images at 0.506 μm. Images were acquired using the 63X objective lens with numerical aperture of 1.4, with immersion oil as the media. Images pixel sizes are indicated in the figure legends.

Allogeneic MLR and proliferation assay

For each assay, freshly isolated PBMCs from two healthy buffy coat donors were used accordingly (Muul et al., 2011). One served as effector cells and the other serve as stimulator cells. Effector cells were labeled with CFSE (1 μM; Invitrogen). Stimulator cells were γ-irradiated at 40 Gy before co-cultured with effector cells at 1:1 ratio for 5 days at 37°C with 5% CO_2. For some experiments, γδ-T cells co-cultured (at 1:1 ratio) with autologous purified naïve or total $CD4^+$ T cells (isolated using negative isolation microbeads kit; Miltenyi Biotec) served as effector cells, in the presence of γ-irradiated PBMCs of an allogeneic donor as stimulators. For CMV-specific response, γδ-T cells purified from CMV-infected PBMCs day 3 P.I. were isolated by microbeads were used as stimulators. Positive control is PHA (5 μg/ml, Sigma-Aldrich) plus IL-2 (40 U/ml, R&D Systems) treated CFSE-labeled PBMCs or T cells, or left untreated as negative control. Anti-Δ42PD1 monoclonal antibody (CH101; 3 μg/ml), anti-TLR4 polyclonal antibody (5 μg/ml; Invivogen) or relevant isotype control antibody was used to pre-treat γδ-T cells or effector PBMCs, respectively, for 30 min at 37°C with 5% CO_2 before added to the co-culture as previous (Cheung et al., 2017).

Co-culture experiments

To generate CMV pp65 antigen-specific $CD4^+$ T cells, freshly isolated PBMCs were first stimulated with PepTivator CMV pp65 (Miltenyi Biotec) according to manufacturer's

instructions and expanded using similar methods as previously described (Brandes et al., 2005). CMV pp65 is also known as pUL83 or glycoprotein B (gB) protein. Briefly, after 3 days of PepTivator CMV pp65 treatment (5 μl/ml), samples that developed colony expansion monitored by light microscopy had 40 U/ml of recombinant human IL-2 (Peprotech) added to the culture. Four days later, γ-irradiated (40 Gy) autologous PBMCs were added at 1:5 ratio and left for another 7 days, with 50% media change replenishing IL-2 every 3 days. To test CMV specific T cell responses, γδ-T cells were purified from CMV-infected PBMC culture at day 3 P.I. by negative selection for co-culture with total $CD4^+$ T cells isolated from these pp65-treated PBMCs for 24 h, and assessed for intracellular IFN-γ.

To generate TT C-fragment antigen-specific $CD4^+$ T cells, similar methods were used as previously described (Brandes et al., 2005). Purified total $CD4^+$ T cells (CD4 Isolation Kit, Miltenyi Biotec) were pulsed with TT C-fragment (10 μg/ml, Santa Cruz) with adding γ-irradiated PBMCs (40 Gy, 1:100), starting from 1×10^6 $CD4^+$ T cells in 100 μL media supplemented with IL-2 (50 U/ml) every three days for two weeks.

To investigate antigen-specific $CD4^+$ T cells response to $\Delta 42PD1^+V\delta 2$ cells, TT C-fragment (1 μg/ml) or pp65/gB recombinant protein (1 μg/ml; Sino Biological) was used to pulse activated γδ-T cells for 24-36 h after stimulation with IPP (50 μM) and IL-2 (50 U/ml) or IL-12 (4 ng/ml) and IL-15 (20 ng/ml) for 18 h; or to MoDCs that was matured with LPS (100 ng/ml) at the last 8 hours before γ-irradiation. Irradiated TT antigen- or pp65- pulsed γδ-T cells or DCs were then co-cultured with respective TT- or pp65- specific $CD4^+$ T cells with ratio of 1:5 overnight and treated with Brefeldin A (10 μg/ml, Sigma) one hour after co-culture. Anti-Δ42PD1 monoclonal antibody (CH101; 3 μg/ml) was used to pre-treat effector γδ-T cells; anti-TLR4 polyclonal antibody (5 μg/ml; Invivogen) or anti-PD-L1 (Nivolumab, 1 μg/ml, MedChemExpress) were used for $CD4^+$ T cells. Relevant isotype control antibodies were used.

Pre-treatment occurred for 30 min at 37°C with 5% CO_2 before added to the co-culture. Cells were harvested and assessed by flow cytometry for IFN-γ expression.

For non-antigen associated co-culture experiments, γδ-T cells were stimulated with IL-12 (4 ng/ml) and IL-15 (20 ng/ml) for 5 days before co-cultured with autologous negatively isolated total $CD4^+$ T cells to assess CFSE proliferation or intracellular IFN-γ expression by flow cytometry. RPMI 1640/10% FBS or AIM-V media (#120550091, Thermo Fisher Scientific) were used. Blocking antibodies against anti-Δ42PD1 were used to pre-treat γδ-T cells or anti-TLR4 used for $CD4^+$ T cells 30 min before co-culture.

Statistical analysis

All statistical analyses were performed using a paired two-tailed Student's t-test or Mann-Whitney U-test to calculate *P* values. $P<0.05$ were considered statistically significant. Data were presented as mean±SEM of at least three independent experiments (n) unless indicated.

Supplemental References

BRANDES, M., WILLIMANN, K. & MOSER, B. 2005. Professional Antigen-Presentation Function by Human gd T Cells. *Science,* 309**,** 264-268.

CHENG, L., TANG, X., LIU, L., PENG, J., NISHIURA, K., CHEUNG, A. K. L., GUO, J., WU, X., TANG, H. Y., AN, M., ZHOU, J., CHEUNG, K. W., WANG, H., GUAN, X., WU, Z. & CHEN, Z. 2015. Monoclonal antibodies specific to human Δ42PD1: A novel immunoregulator potentially involved in HIV-1 and tumor pathogenesis. *MAbs,* 7**,** 0.

CHEUNG, A. K. L., ABENDROTH, A., CUNNINGHAM, A. L. & SLOBEDMAN, B. 2006. Viral gene expression during the establishment of human cytomegalovirus latent infection in myeloid progenitor cells. *Blood,* 108**,** 3691-3699.

CHEUNG, A. K. L., KWOK, H. Y., HUANG, Y., CHEN, M., MO, Y., WU, X., LAM, K. S., KONG, H. K., LAU, T. C. K., ZHOU, J., LI, J., CHENG, L., KIAT LEE, B., PENG, Q., LU, X., AN, M., WANG, H., SHANG, H., ZHOU, B., WU, H., XU, A., YUEN, K. Y. & CHEN, Z. 2017. Gut-homing Delta42PD1(+)Vdelta2 T cells promote innate mucosal damage via TLR4 during acute HIV type 1 infection. *Nat Microbiol,* 2**,** 1389-1402.

COSTES, S. V., DAELEMANS, D., CHO, E. H., DOBBIN, Z., PAVLAKIS, G. & LOCKETT, S. 2004. Automatic and quantitative measurement of protein-protein colocalization in live cells. *Biophys J,* 86**,** 3993-4003.

KANG, Y., WU, Z., LAU, T. C. K., LU, X., LIU, L., CHEUNG, A. K. L., TAN, Z., NG, J., LIANG, J., WANG, H., LI, S., ZHENG, B., LI, B., CHEN, L. & CHEN, Z. 2012. CCR5 antagonist TD-0680 uses a novel mechanism for enhanced potency against HIV-1 entry, cell-mediated infection, and a resistant variant. *J Biol Chem,* 287**,** 16499-16509.

MUUL, L. M., HEINE, G., SILVIN, C., JAMES, S. P., CANDOTTI, F., RADBRUCH, A. & WORM, M. 2011. Measurement of proliferative responses of cultured lymphocytes. *Current protocols in immunology / edited by John E. Coligan ... [et al.],* Chapter 7**,** Unit7.10.

SCHNEIDER, C. A., RASBAND, W. S. & ELICEIRI, K. W. 2012. NIH Image to ImageJ: 25 years of image analysis. *Nature methods,* 9**,** 671-675.